

## **Copyright Warning & Restrictions**

The copyright law of the United States (Title 17, United States Code) governs the making of photocopies or other reproductions of copyrighted material.

Under certain conditions specified in the law, libraries and archives are authorized to furnish a photocopy or other reproduction. One of these specified conditions is that the photocopy or reproduction is not to be “used for any purpose other than private study, scholarship, or research.” If a user makes a request for, or later uses, a photocopy or reproduction for purposes in excess of “fair use” that user may be liable for copyright infringement,

This institution reserves the right to refuse to accept a copying order if, in its judgment, fulfillment of the order would involve violation of copyright law.

**Please Note: The author retains the copyright while the New Jersey Institute of Technology reserves the right to distribute this thesis or dissertation**

Printing note: If you do not wish to print this page, then select “Pages from: first page # to: last page #” on the print dialog screen

The Van Houten library has removed some of the personal information and all signatures from the approval page and biographical sketches of theses and dissertations in order to protect the identity of NJIT graduates and faculty.

## **ABSTRACT**

### **NON-INVASIVE MONITORING OF BONE HEALTH USING ULTRASOUND**

**by  
Nashit Jahan Meem**

Bone fractures are estimated to afflict everyone at least once in his/her lifetime. Monitoring this becomes crucial especially when it comes to athletes in order for them to safely resume their regular activities as soon as possible. Technologies currently employed are either very expensive or use harmful radiation.

Ultrasound can monitor bone fractures in a non-invasive manner, as discussed in United States Patent # 5143069. Three transducers are mounted over the test specimen. A pulse generator excites the transmitting receiver. The second receiver is mounted next to the transmitter and acts as a reference receiver that displays the response across a normal area. The third transducer is mounted across the area suspected to have some defect and acts as the sample receiver to display the response across the discontinuity. Both the received signals are viewed on a dual channel digital oscilloscope, saved onto a diskette and processed for data analysis by quantifying parameters such as flight time and amplitude.

Experiments were conducted on mock bones (wood and metal), cow bone with some meat on it, the human arm and the human tibia. Discontinuity in the first two test specimens resulted in rise in flight time and loss of amplitude. Results from the other three experiments displayed two packets of signals, the first packet corresponding to bone and the second to the soft tissue around it.

**NON-INVASIVE MONITORING OF BONE  
HEALTH USING ULTRASOUND**

by  
**Nashit Jahan Meem**

**A Thesis  
Submitted to the Faculty of  
New Jersey Institute of Technology  
On Partial Fulfillment of the Requirements for the Degree of  
Master of Science in Biomedical Engineering**

**Department of Biomedical Engineering**

**January 2006**

**APPROVAL PAGE**

**NON-INVASIVE MONITORING OF BONE  
HEALTH USING ULTRASOUND**

**Nashit Jahan Meem**

---

**Dr. Michael Jaffe, Thesis Advisor** **Date**  
Research Professor, Biomedical Engineering Department, NJIT

---

**Mr. Sanford A. Roth, Committee Member** **Date**  
President & CEO, Medsonics US, Inc.

---

**Dr. Richard A. Foulds, Committee Member** **Date**  
Associate Professor, Biomedical Engineering Department, NJIT

## **BIOGRAPHICAL SKETCH**

**Author:** Nashit Jahan Meem

**Degree:** Master of Science

**Date:** January 2006

### **Undergraduate and Graduate Education:**

- Master of Science in Biomedical Engineering,  
New Jersey Institute of Technology, Newark, NJ, 2006
- Bachelor of Science in Biomedical Engineering,  
Rutgers University, New Brunswick, NJ, 2004

**Major:** Biomedical Engineering

To my beloved parents and brother who supported me throughout this endeavor

## ACKNOWLEDGEMENT

I would like to express my sincere gratitude to Dr. Michael Jaffe for his faith, encouragement and guidance, throughout this research.

Special thanks to Mr. Sanford Roth who has been guiding and helping me throughout my thesis and actively participating in my committee.

I would like to thank Dr. Richard Foulds for his valuable suggestions and encouragement.

I also wish to thank Dr. Jason Steffener for guiding me and helping me with experimental and technical work; Dr. Glenn Kashan for his valuable input; Mr. Joseph Pickton, laboratory manager of the Medical Device Concept Laboratory, for managing to get us cow bone; and Mrs. Jean Collins for always seeing to my other needs around the lab.

Last, but not least, I would like to thank my family, for their assistance and constant belief in my abilities and their support over the years.



## TABLE OF CONTENTS

Chapter	Page
1 INTRODUCTION.....	1
2 BACKGROUND.....	2
2.1 Bone – General Overview.....	2
2.2 Bone – Anatomical Overview .....	2
2.3 Bone Structure.....	4
2.4 Bone Fracture.....	4
2.4.1 Symptom of a Bone Fracture.....	5
2.4.2 Types of Fractures.....	5
2.5 Bone Healing Physiology .....	6
3 RESEARCH OBJECTIVE.....	8
4 WORKING PRINCIPLE.....	9
4.1 Ultrasound.....	9
4.2 Why Ultrasound?.....	10
4.3 Current Technology.....	11
4.4 Advantage of this Study over Current Technology.....	12
5 DEVICE DESIGN.....	14
5.1 Experimental Setup.....	14
5.2 Transducers.....	14
5.3 Pulse Generator.....	16
5.4 Oscilloscope.....	16

**TABLE OF CONTENTS**  
**(Continued)**

<b>Chapter</b>	<b>Page</b>
5.5 BNC Cables.....	17
5.6 Gel.....	18
6 EXPERIMENTAL APPROACH.....	19
6.1 Methods.....	19
6.2 Experiments.....	21
6.2.1 Transducers: Face to Face Coupling to allow Calibration.....	21
6.2.2 Experiments on Wood.....	22
6.2.3 Experiments on Metal.....	22
6.2.4 Experiments on Cow Bone.....	22
6.2.5 Experiments on Human Arm.....	23
6.2.6 Experiments on Human Tibia.....	23
7 RESULTS AND DISCUSSION.....	24
7.1 Results for Input Signal.....	26
7.2 Results for Wood.....	27
7.2.1 Wood without Cut versus Wood with Cut.....	27
7.2.2 Dowel of Wood and Wood with Knot.....	31
7.3 Results for Metal.....	33
7.4 Results for Cow Bone.....	37
7.5 Results for Human Arm.....	39
7.6 Results for Human Tibia.....	43

**TABLE OF CONTENTS**  
**(Continued)**

<b>Chapter</b>	<b>Page</b>
7.7 Result Summary.....	45
8 CONCLUSION.....	46
9 DRAWBACKS - NEEDS FOR THE NEXT GENERATION INSTRUMENT.....	49
10 RECOMMENDATIONS AND FUTURE WORK.....	50
REFERENCES .....	51

## LIST OF TABLES

<b>Table</b>	<b>Page</b>
7.1    Ultrasound Velocity through Test Specimens.....	25

## LIST OF FIGURES

Figure	Page
2.1 Structure of bone.....	4
4.1 Particle motion versus direction of wave propagation in ultrasonic waves.....	9
4.2 Block diagram of US Patent # 5143069 signal processing procedure.....	10
5.1 Structure of an ultrasound transducer.....	15
5.2 Pulse generator.....	16
5.3 Digital oscilloscope.....	17
5.4 BNC-BNC cable.....	17
6.1 Block diagram for the sonic diagnostic method.....	20
6.2 Setup for input signal.....	21
6.3 Experimental setup for control.....	23
6.4 Experimental setup for material with defects.....	23
7.1 Input signal waveform.....	26
7.2 Overlapping waveforms for test on wood with no cut.....	27
7.3 Overlapping waveforms for test on wood with cut.....	27
7.4 Separated signals for test on wood with no cut.....	28
7.5 Separated signals for test on wood with cut.....	28
7.6 Cross-correlation of received signals for wood with no cut.....	29
7.7 Cross-correlation of received signals for wood with cut.....	29
7.8 Reference and received signals for wood with a knot on it.....	31
7.9 Reference and received signals for a dowel of hardwood.....	31

**LIST OF FIGURES**  
**(Continued)**

<b>Figure</b>	<b>Page</b>
7.10 Overlapping waveforms for test on metal without hole.....	33
7.11 Overlapping waveforms for test on metal with hole.....	33
7.12 Separated signals for test on metal without hole.....	34
7.13 Separated signals for test on metal with hole.....	34
7.14 Cross-correlation of received signals for metal without hole.....	35
7.15 Cross-correlation of received signals for metal with hole.....	35
7.16 Received signal for cow bone with no pressure applied around transducers.....	37
7.17 Received signal for cow bone with pressure applied around transducers.....	37
7.18 Overlapping waveforms for test for arm with no pressure applied.....	39
7.19 Overlapping waveforms for test for arm with pressure applied.....	39
7.20 Separated signals for test on human arm with no pressure applied.....	40
7.21 Separated signals for test on human arm with pressure applied.....	40
7.22 Cross-correlation of received signals for arm with no pressure.....	41
7.23 Cross-correlation of received signals for arm with pressure applied.....	41
7.24 Overlapping waveforms for test on the human tibia.....	43
7.25 Separated signals for test on the human tibia.....	43
7.26 Cross-correlation of received signals for tibia.....	44
7.27 Cross-correlation of input and far received signals for tibia.....	44
7.28 Illustration of how delta parameter changes in the healing process.....	45
7.29 Graphical representation of change in parameter with and without defect.....	46

## LIST OF DEFINITIONS

T	Transmitting
R	Receiving
XMTR	Transmitter
REF	Reference
RCVR	Receiver
EXT. TRIGG	External Trigger
CH1	Channel 1
CH2	Channel 2

# CHAPTER 1

## INTRODUCTION

*“A runner stumbles and twists an ankle. A soldier cracks his elbow. An old man falls off the stairs. A little kid falls off monkey bars. Did they encounter with a fracture? If so, how intense is the fracture? How fast is it healing? Is there a way to monitor this non-invasively or without using techniques such as x-ray?”*

The skeletal system is of great importance in deciding overall suitability for a sport and performance within some sports. The structural response of hard connective tissues has been studied considerably due to the clinical importance of providing information about specific bone mechanical properties.

Techniques that employ impedance, resonance and acoustic emission have not been widely accepted for assessing in-vivo properties of bones due to the effects of adjacent bones, muscles, ligaments and associated tissues that hinder the precise mounting of sensors, thereby affecting the responses. In contrast, ultrasound energy can be separated from the surrounding soft tissues, thereby allowing unbiased, precise determination of ultrasound parameters that represent bone health [10].

The main goal of this study is

- To demonstrate an ultrasound technique for the real time monitoring of discontinuity in long bones.
- To validate the methods described in United States Patent # 5143069 as the technological basis of the demonstration.

This would, in turn, pave the way for developing a portable, cost effective, point of care bone health monitoring device using advanced digital ultrasound technology.



## **CHAPTER 2**

### **BACKGROUND**

#### **2.1 Bone – General Overview**

Bone is a unique tissue because it is continuously metabolically active and thus subject to a variety of systemic and local factors throughout life. Bone is a tissue that constantly undergoes deposition, resorption of stromal matrix (the supporting tissue framework within which cells are embedded), and remodeling [3]. These processes may be altered by a variety of chemical, mechanical, cellular, and pathological mechanisms. Understanding the physiology of bone healing and the mechanisms affecting this process is important not only when evaluating normal skeletal development but also when initiating fracture repair. Because the ultimate success of spinal fusions involves creation of an osseous union, the following overview sheds some light on the anatomy of bone under physiological conditions, normal bone healing and mechanisms that alter it, and available adjuvant therapies (treatments given after the primary treatment) that may enhance healing potential in a clinical setting [6].

#### **2.2 Bone – Anatomical Overview**

The skeletal system in the human body is made up of 206 bones [6]. In normal children, the bones account for almost twenty percent of their total body weight. Such is the importance of bones in various sports that there is a large body of data concerning ideal bone and skeletal system dimensions for the various sports. In fact it is actually a science called Kinanthropometrics [4].

There are three main areas of consideration for the role that the skeletal system plays in athletic performance. They are as follows:

1. Overall size of the skeleton
2. The skeleton's proportions
3. The size of certain crucial individual bones.

The overall size of the skeleton refers mainly to the total height of the body. Proportion refers to the size of the upper body or trunk relative to the lower body or legs. Being an important factor in determining center of gravity, the proportion of the skeleton is a more important variable in most sports than its overall size. A low center of gravity is critical to the performance of a number of sports, especially those requiring upright balance (i.e. skiing) or balance during tumultuous movement (i.e. football offensive backfield). Conversely, a high center of gravity is important to runners. The longer the upper body is in relation to the lower body, the lower the center of gravity.

The importance of the size of individual bones is entirely dependent upon the sport under consideration. Certain sports are advantageous to individuals with certain length body parts. Boxers, for example, need long arms. This is called "reach" [6]. Swimmers benefit from large hands and wide feet. The sport of running favors those with long thighs while sprinters need a narrow pelvis which allows for a more direct line for the legs to follow. In general, the size of the individual body parts are far better determinants for ease of success in a given sport than is the overall height of the skeleton.

### 2.3 Bone Structure

Almost every bone in the body has the same structure. The outer surface of bone is called the **periosteum**. It is a thin, dense membrane that contains nerves and blood vessels that nourish the bone [5].

The next layer is made up of **compact** bone. This part is smooth and very hard. Many layers of **cancellous** bone are found within the compact bone. In spite of its spongy looks, it is still very strong.

The cancellous bone protects the innermost part of the bone, the **bone marrow**, which is thick, jelly-like, and makes blood cells.

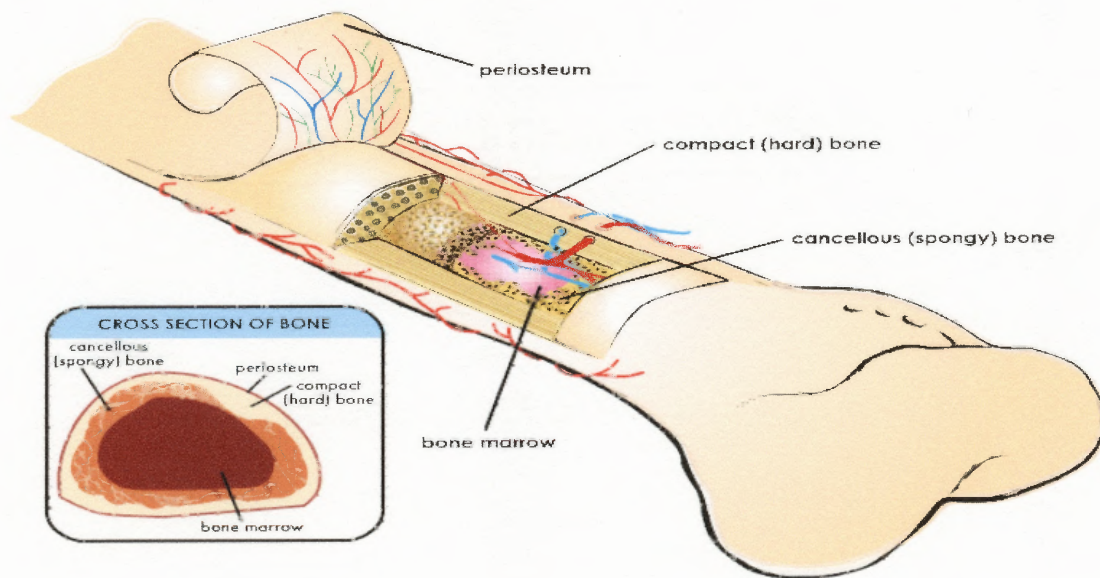


**Figure 2.1** Structure of bone [5].

### 2.4 Bone Fracture

A bone fracture is a medical condition in which a bone becomes cracked, splintered, or bisected as a result of physical trauma. Fractures are common. It is not uncommon to find people fracturing at least one bone during their lifetime. The severity of fractures

increases with age. Children have more flexible bones that are less likely to break. Falls or other accidents that do not harm children can cause complete fractures in older adults. Older adults suffer from fractures more than children because their bones are more likely to be brittle. Fractures occur when a bone cannot withstand the physical force exerted on it.

#### **2.4.1 Symptoms of a Bone Fracture**

The most common symptoms are [2]:

- swelling around the injured area
- loss of function in the injured area
- bruising around the injured area
- deformity of a limb

#### **2.4.2 Types of Fractures**

There are many types of fractures: simple, stress, comminuted, impacted, compound, complete and incomplete [2].

1. Simple: Bone breaks into two pieces.
2. Stress: Hairline break that is often invisible on the x-ray for the first six weeks.
3. Comminuted: Bone fragments into several pieces.
4. Impacted: One fragment of bone is embedded into another fragment of bone.
5. Compound (Open): Bone protrudes through the skin.
6. Complete: Bone snaps completely into two or more pieces.
7. Incomplete: Bone cracks but does not separate.

## 2.5 Bone Healing Physiology

There are five phases of bone healing:

1. Fracture and Inflammatory Phase
2. Granulation Tissue Formation
3. Callus Formation
4. Lamellar Bone Deposition
5. Remodeling

The natural process of healing a fracture starts when the injured bone and surrounding tissues bleed. The blood coagulates to form the haematoma, which is a clot of blood originating from the lacerated blood vessels in the bone and the periosteum. Necrotic bone is then resorbed by osteoclasts (multinucleated cells that degrade and reabsorb bone), and the haematoma by macrophages [3]. This is followed by development of a tissue, containing collagen and fibroblasts, from the periosteum and endosteum to replace the healing tissue. This paves the way for the migration of pluripotent cells that eventually become chondrocytes and later osteocytes, that produce cartilage and bone respectively. The structure surrounding the fracture site is now slightly harder and is a provisional callus. The area can be called a proper callus as time goes on, and more and more woven bone is made by the osteoblasts (mononucleate cells that produce a protein called osteoid.). This initial "woven" bone does not have the strong mechanical properties of mature bone. By a process of remodelling, the woven bone is replaced by mature "lamellar" bone. The callus becomes smaller, as the trabeculae are formed along lines of stress [3]. The whole process can take up to 18 months, but in

adults the strength of the healing bone is usually 80% of normal by 3 months after the injury.

### **CHAPTER 3**

#### **RESEARCH OBJECTIVE**

The main objective of this study is to show proof of concept of the ultrasound device defined by United States Patent # 5143069 by using more sophisticated and modern signal processing procedures. This would ensure the following:

- Quantitative measurement of the in-vivo mechanical integrity of bone in a non-invasive and non-traumatic environment.
- Very simple data treatment methodology.
- High efficacy in detecting responses from both bone and soft tissue surrounding it.
- High efficacy in detecting discontinuity along long bones.
- Monitoring the rate of the bone healing process.

## CHAPTER 4

### WORKING PRINCIPLE

#### 4.1 Ultrasound

Ultrasound is based on sound waves generated above the human hearing range, about 20 KHz. Frequency ranges from 100 KHz to 50 MHz are employed when ultrasound is used for testing purposes.

Ultrasound waves travel just like light waves except for the fact that they require an elastic medium such as a liquid or a solid and they cannot travel in vacuum. Ultrasound velocity in a perfectly elastic material at a given temperature and pressure is constant. The velocity is a function of the material modulus and structural uniformity.

Longitudinal waves and shear waves are the common methods of examining ultrasound propagation. The longitudinal wave is a compressional wave in which the particle motion is in the same direction as the propagation of the wave [1]. The shear wave is a wave motion in which the particle motion is perpendicular to the direction of propagation [1]. This is illustrated in Figure 4.1 below.

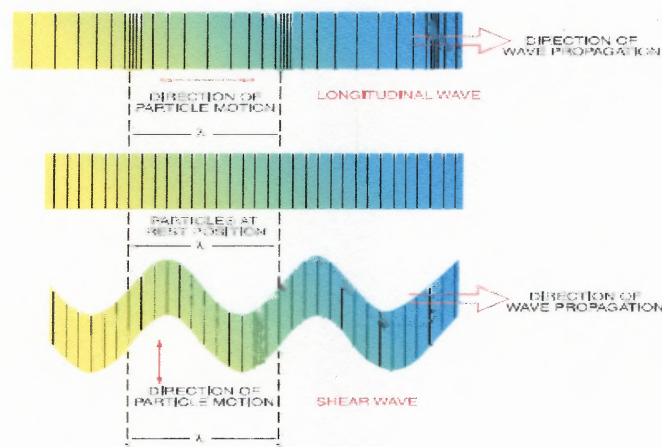


**Figure 4.1** Particle motion versus direction of wave propagation in ultrasonic waves [1].



## 4.2 Why Ultrasound?

The basis of this study, the United States Patent # 5143069, was released in 1982. It is titled “Diagnostic Method of Monitoring Skeletal Defect by In-Vivo Acoustic Measurement of Mechanical Strength using Correlation and Spectral Analysis”. Seo J. Kwon and Lawrence Katz were the inventors of this technique in the 80’s. The patent claims the measurement of in-vivo mechanical strength and structural integrity of hard and soft tissues by relating them to velocity, propagation energy and degree of dispersion of ultrasound signal propagated along bones and surrounding soft tissues. The following block diagram illustrates the procedure defined in the patent.

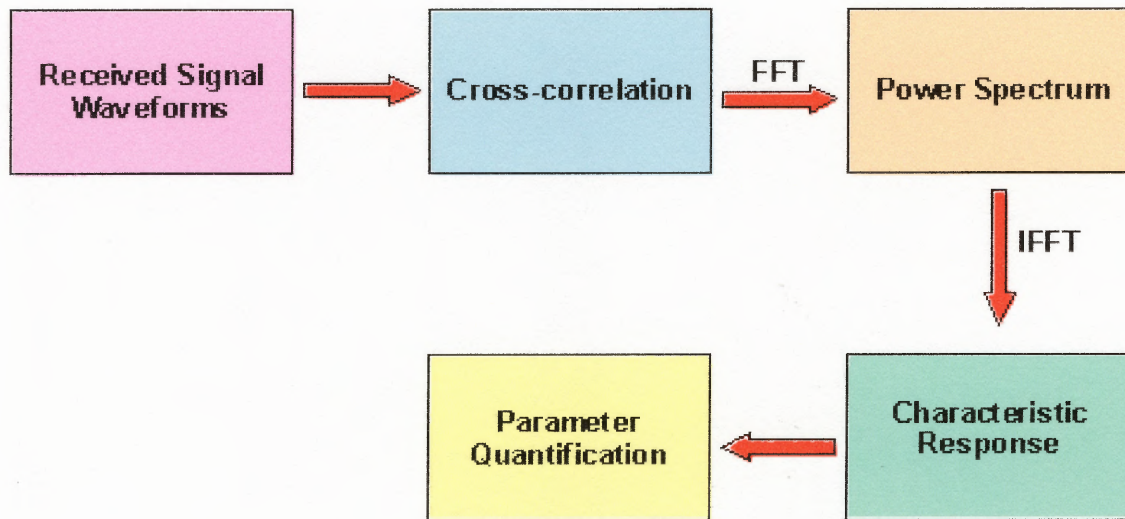


**Figure 4.2** Block diagram of US Patent # 5143069 signal processing procedure.

There are certain kinds of bone damage that x-rays simply overlook, for example, stress fractures [11]. “Unlike x-rays, sound doesn’t just scan or photograph the surface of a bone. Sound waves penetrate the bone tissue and can even detect a single splintered

fiber,” says Hyo Sub Yoon, a biomedical engineer from the Rensselaer Polytechnic Institute in Troy, New York [11].

Ultrasonic measurements can be very sensitive to any micro structural change in bone. This is attributed to its short wavelength that enables it to reflect off very small surfaces such as defects inside materials. Ultrasound can diagnose bones by “listening” to them, including all abnormalities in the resulting signal [11]. This is done by sending a high frequency sound wave from a transmitting transducer to a receiving transducer across the bone area where the fracture is suspected to have occurred. The same signal is sent over a normal section of bone, providing a healthy bone reference signal. The quantitative difference between healthy and damaged bone response corresponds to the degree of bone damage or discontinuity.

### **4.3 Current Technology**

A number of techniques such as x-ray imaging, dual photon absorbtometry, scintigraphy, CT scanning (x-ray and ultrasonic) and MRI are currently in use for diagnosing bone disorders. However, they are only sensitive to mineral density changes and not very sensitive to the mechanical strength of hard tissues [16].

To discuss these techniques in brief, x-ray imaging uses ionizing radiation to image internal structures of the body. X-ray CT scanning uses special x-ray equipment to obtain many images from different angles and then join them together to show a cross-section of body tissues and organs. Dual photon absorptiometry measures bone mineral content by comparing the transmission of the two separate photoelectric energy peaks (44 and 100 keV) emitted by gadolinium-153, a magnetic metallic element of the rare-earth

group, through both soft and bone tissues [16]. Scintigraphy is another diagnostic technique that uses a gamma camera to obtain two-dimensional picture of a bodily radiation source[4]. Radioisotopes when injected into the body lead to selective accumulation in specific tissues. In the case of bone, technetium-99 is used. All these techniques employ ionizing radiation, which poses a threat to the patients since it can lead to genetic defects in future generations or even fatal cancer.

Ultrasonic CT scanning produces an image by computed tomography using two transducers, a transmitter and a receiver, that can be rotated around the test area. MRI produces detailed images of internal organs by using a combination of a large magnet, radio frequencies, and a computer. Although these two techniques use non-ionizing radiation and are useful for detecting soft tissue abnormalities, their resolution for imaging bone is known to be very poor at present [16].

#### **4.4 Advantage of this Study over Current Technology**

The use of ultrasound makes the device:

- non-invasive
- non-hazardous
- non-traumatic
- allow frequent monitoring
- simple to use by paramedical personnel

When compared to techniques such as CT and MRI devices that use large machines, the use of ultrasound has the following advantages:

- a) Ultrasound devices are a fraction of the cost of CT and MRI devices which cost over a million dollars.

- b) They cost much less per procedure.
- c) They do not expose the patient to hazardous radiation.
- d) They allow for real-time diagnosis.
- e) They provide direct information of the mechanical properties of bone.
- f) If made portable, they can be brought to the patient, in the hospital, home, office or battlefield.

Mechanical properties of bones constitute an important function of bone. Because it measures these properties directly, ultrasonic wave propagation techniques are advantageous over other bone density measurement and related techniques. In monitoring fracture healing, it is more critical to understand when the bone is at risk of fracture or re-fracture, rather than just how large the bone density or stiffness is [16]. Correlation of bone density, stiffness and bone strength is rather difficult. Ultrasound therefore has great potential to overcome these hurdles, along with high precision and low cost.

Therefore, the aim of this study is focused on diagnosing and monitoring bone fractures and micro-fractures, healing rate, identification of non-unions and osteoporosis. It also has the potential to diagnose the surrounding soft tissues and internal organ damage and possibly cancerous growths, radiolucent and metallic foreign matter and even the pathological state prediction of abnormalities. However, the main focus of this study is exclusively on bones.

## **CHAPTER 5**

### **DEVICE DESIGN**

#### **5.1 Experimental Setup**

Based on the experimental setup described in the referenced patent [22], three ultrasound transducers are mounted over the skin of a living human or on a mock bone (wood, metal, etc.). The ultrasound signal propagates along the hard tissues and surrounding soft tissues or along the length of the mock bone. One transducer acts as the transmitter while the other two act as receivers. The first receiver is used to establish a fixed reference signal for the normal portion of bone whereas the second receiver is the sample receiver that establishes a propagated ultrasound signal. The reference receiver is mounted next to the transmitter and the sample receiver is mounted across the suspected fractured site [18].

The increased utility of the device (from patent [22] examples) is enabled by using more sensitive transducers and a more sophisticated pulse generator (with built-in amplifier and filters). This also enables the miniaturization of the setup when compared to the setup used in the earlier experiments.

#### **5.2 Transducers**

A transducer is a device that converts one form of energy into another. An ultrasound transducer converts electrical energy to mechanical energy in the form of sound and vice versa. It is made up of three main components – the active element, backing, and wear plate [1]. The active element converts an excitation pulse (electrical energy) into ultrasonic energy and is a piezoelectric or ferroelectric material. A piezoelectric material

exhibits electric polarity due to pressure especially in a crystalline substance whereas a ferroelectric material shows spontaneous electric polarization reversible by an electric field [4]. The backing is a highly attenuative, high-density material that controls the vibration of the transducer by absorbing the energy radiating from the back face of the active element. The wear plate protects the transducer from the testing environment and therefore, must be durable and corrosion resistant.

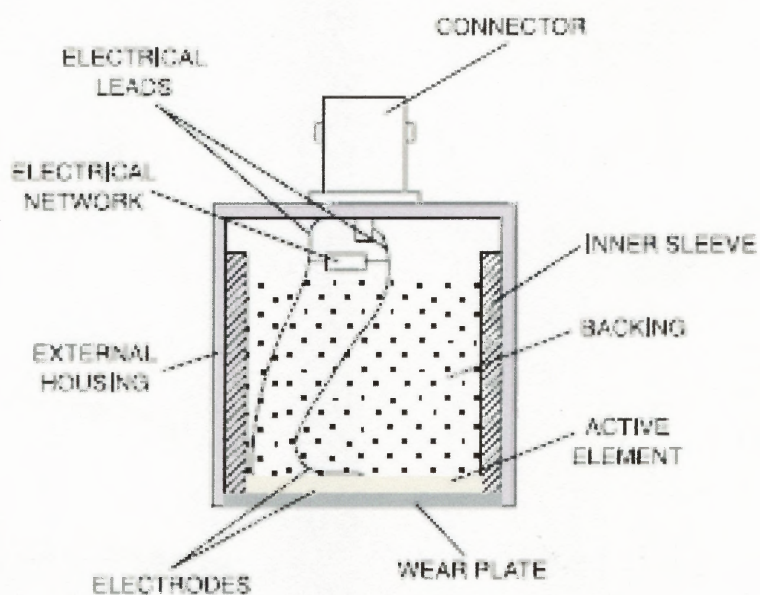


**Figure 5.1** Structure of an ultrasound transducer [1].

The transducers used in this research were high sensitivity piezoelectric transducers with nominal center frequency 500 kHz and bandwidth 97.98%, which implies that they emit frequencies from 250-750 kHz approximately. They were contact videoscans transducers (Model# V101, Panametrics Inc.) and one inch in diameter.



### 5.3 Pulse Generator

A pulse generator is used to generate single or multiple voltage pulses that can then be injected into a device under test and used as a stimulus or analyzed as they progress through the device, confirming the proper operation of the device or pinpointing a fault in the device.

The pulse generator used in this research was an ultrasonic pulser-receiver (Panametrics 5072PR) that is designed to provide the high energy, high gain performance necessary for low frequency investigation of attenuating materials. It is ideal for thin materials analysis and high resolution flaw detection. The frequency range in which the transducers are excited is 100 Hz to 5000 Hz. Energy ranges from 13  $\mu$ joules to 104  $\mu$ joules and damping ranges from 15 ohms to 500 ohms. The gain could be adjusted between -59 dB and +59 dB.



**Figure 5.2** Pulse generator.

### 5.4 Oscilloscope

The oscilloscope is basically a graph-displaying device - it draws a graph of an electrical signal. The graph shows how signals change over time: the vertical (Y) axis represents voltage and the horizontal (X) axis represents time. The intensity or brightness of the

display is sometimes called the Z axis. The Agilent 54622A oscilloscope was used in this research. It is a 100 MHz dual channel digital oscilloscope i.e, it has a sampling rate of 200 Megasamples per second.

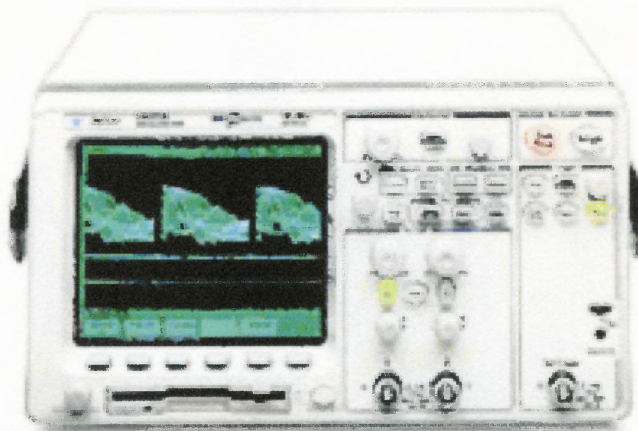


**Figure 5.3** Digital oscilloscope.

### 5.5 BNC Cables

The experimental set up is completed by using BNC cables to connect the pulse generator to the digital oscilloscope. They are heavily shielded and have a ferrite core to provide the highest quality image in ultra high resolution modes.



**Figure 5.4** BNC-BNC cable.



## 5.6 Gel

Ultrasound gel is used for impedance matching which enables the generation of stronger signals. In other words, it is acoustically matched to the frequency range for ultrasound experiments of this research.

For this research, the Grafo ultrasound transmission gel was used. It is a non-greasy water-soluble gel and is an efficient ultrasound coupling medium for diagnostic and therapeutic ultrasonic procedures. It does not stain clothing, damage transducers or irritate skin. It also minimizes refraction through the skin while optimizing coupling.

## CHAPTER 6

### EXPERIMENTAL APPROACH

#### 6.1 Methods

The pulse generator excites the transmitting transducer to transmit ultrasound pulses and then to receive the echoes bouncing back from the front and the rear boundaries of the bone tissues. As mentioned earlier, the transmitting transducer and the reference receiver are mounted next to each other and the sample receiver across the reference receiver. Voltage adjustments were made in order to view the response from both transducers on a relative scale.

A digital oscilloscope with sampling rate of 200 Mega Samples per second was used to view the signals. The experimental setup is as shown in Figure 6.1. The reference receiver is connected to channel 1 of the digital oscilloscope whereas the transmitter and the sample receiver are connected to the pulse generator. The pulse generator with the built-in amplifier greatly amplified only the second received signal. This was necessary since in order to view the sample received signal properly since it was expected to be attenuated to a large extent as opposed to the reference signal. The transmitter and receivers were synchronized by external triggering where BNC cables were used to connect the 'external trigger' slot of the oscilloscope to the 'sync out' slot of the pulse generator. Finally, the other slot in the pulse generator, 'RF out' which acts as the signal output connector for the received signal, was connected to channel 2 of the oscilloscope.

Both received signals are viewed simultaneously on the dual channel digital oscilloscope. The digitized signals were saved in a diskette and opened with a computer

for signal processing. MATLAB was used to cross-correlate the two received signals in order to accumulate and average them to produce a meaningful output from even a very low level input ultrasound.

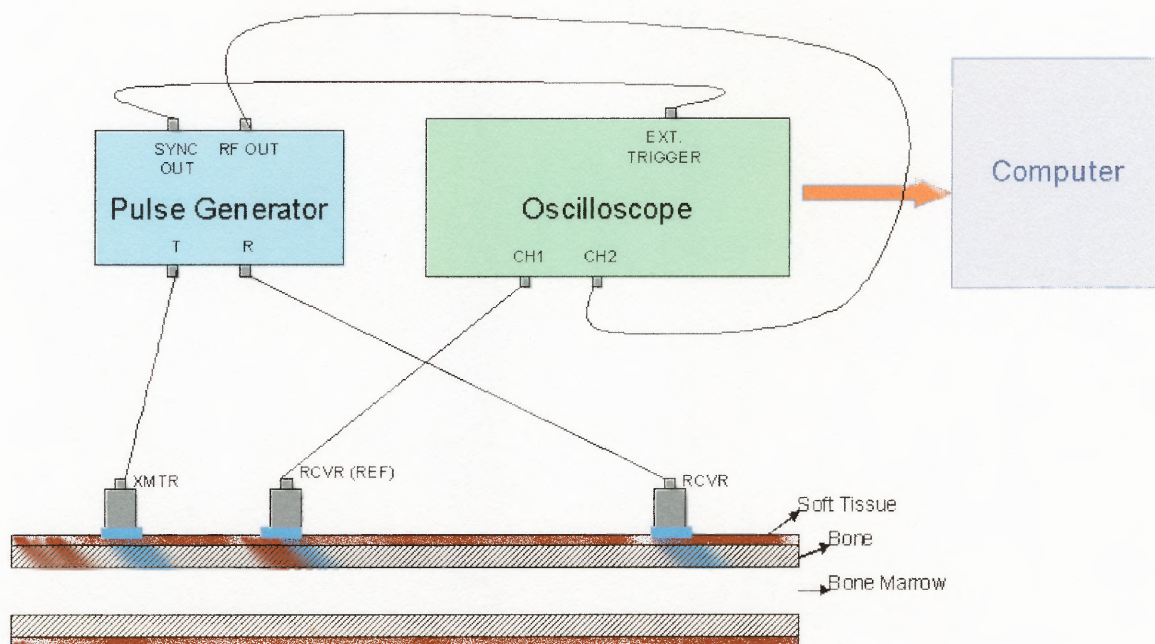


**Figure 6.1** Block Diagram for the sonic diagnostic method.

Cross-correlation is a measure of the similarity of two signals, commonly used to find features in an unknown signal by comparing it to a known one (in this case, to find how much the far receiver signals change from the reference receiver signals). It is a function of the relative time between the signals and is sometimes called the sliding dot product [4]. It is a differential processing technique that is used to illustrate how the 'delta parameter' (such as change in flight time, amplitude, velocity or propagated energy) of a particular response varies with change in material continuity. In the cases when testing is done on the human arm and on the human tibia, cross-correlating serves

to separate out the bone response from the soft tissue response to a certain extent, which in turn facilitates proper processing of the signals.

The transducers were always mounted with sufficient amount of gel to ensure appropriate coupling. The spacing between the transducers is noted. Flight time is obtained from analysis of the responses. It is measured as the time from the start of the pulse to the highest peak in the response. Transducer spacing and flight time are the two parameters used to calculate the velocity of ultrasound in the test specimen. These values are then compared to known velocities of ultrasound through that material for further confirmation of proof of principle. Velocity was calculated by using the simple formula,  $\text{Ultrasound velocity in the test specimen} = (\text{Transducer spacing})/(\text{Flight time})$ .

## 6.2 Experiments

### 6.2.1 Transducers: Face to Face Coupling to allow Calibration

The input ultrasound signal was studied by coupling the transmitter and one of the receivers face to face with sufficient amount of gel, and analyzing the response on the digital oscilloscope. This is done in order to analyze the received ultrasound signal.

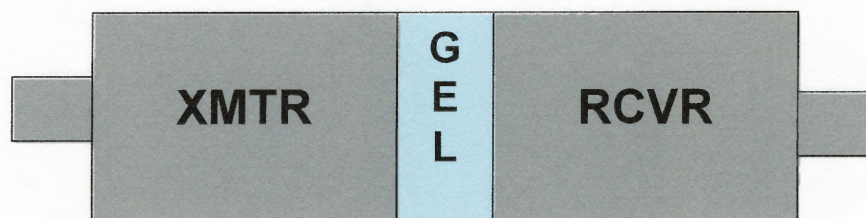


**Figure 6.2** Setup for input signal.

### **6.2.2 Experiments on Wood**

The setup as described above was used to view the responses from a long block of hardwood (pine), 43 cm x 3 cm x 0.7 cm. This block of wood was analyzed for three, well-defined cases. Firstly, the two receivers were placed across a smooth surface of wood. Then they were placed across a cut 0.2 cm deep along the piece of wood. And finally, the second receiver was placed across a knot on the piece of wood. The results were then compared in all three cases. The experiment was also conducted on a dowel of hardwood in which case, the two surfaces (transducer and test specimen) were not in complete contact. The alignment was always transmitter-receiver-receiver and the spacing between the transmitter and far receiver was 8.7 cm.

### **6.2.3 Experiments on Metal**

Two cases were studied with a block of aluminum measuring 40 cm x 12.5 cm x 1.2 cm. The transducers were first placed over a smooth surface and then the two receivers were placed across a defect on the aluminum block i.e, across a hole 0.5 cm in diameter. The results were then processed and analyzed. The spacing between the transmitter and far receiver was 9.5 cm.

### **6.2.4 Experiments on Cow Bone**

Experiments similar to that on the piece of wood were conducted over the tibia of a cow – with cut and without cut, and the results analyzed accordingly. The transducers were spaced 5.1 cm apart.



### 6.2.5 Experiments on a Human Arm

The transducers were mounted on the human arm to study the responses for both bone as well as soft tissue. Two cases were studied – one in which the soft tissue around the transducers is not disturbed and the other in which pressure is applied on the soft tissues surrounding the transducers. This is done to illustrate separation of signals between bone and soft tissue. The transmitter and far receiver were spaced 12.7 cm apart.

### 6.2.6 Experiments on a Human Tibia

In order to test for reproducibility, the experiment was conducted on the human tibia as well. The transmitter and far receiver were spaced 19.1 cm apart.

Figures 6.3 and 6.4 show the general setup of the experiments pictorially. The area being diagnosed is always the area across the two receivers.

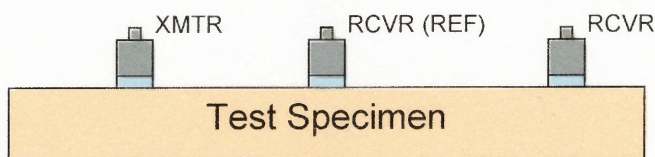


**Figure 6.3** Experimental setup for control.

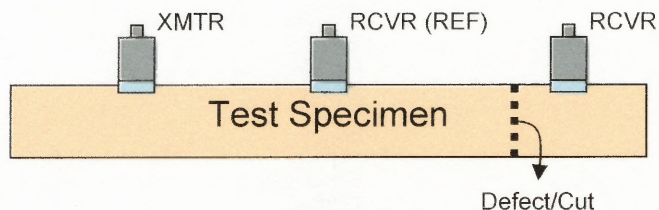


**Figure 6.4** Experimental setup for material with defects.

## CHAPTER 7

### RESULTS AND DISCUSSION

Very interesting results have been observed in each of the experiments conducted with the demonstration device. The two parameters used to quantify the results are flight time and amplitude. Flight time is the time it takes the ultrasound signal to propagate through the material and is measured as the time delay from the start of the pulse to the highest peak in the signal. This method was used on the basis of the flight time determination method defined by the referenced patent [22]. The amplitude of the received signal is a simple measure of the voltage of the received signal along the y-axis.

The change in these two parameters was observed for all the different experiments that were conducted. In all the experiments, defects or cuts along the test specimen showed sharp increases in flight time whereas the amplitude went down in those cases. Application of pressure however, caused increase in amplitude of the received signal.

It was observed that sufficient gel must be used to ensure efficient coupling of the transducers with the test specimen. This also eliminates the unwanted noise signal to a large extent. Reproducibility has been observed as a result of consistent results for defects versus no defect and pressure versus no pressure applied. With cross-correlation, this principle maximizes the differences in the responses.

The calculated ultrasound velocities for wood, aluminum and cow bone approximately match the known ultrasound velocity through these materials, respectively. Table 7.1 summarizes the velocity calculations.

**Table 7.1** Ultrasound Velocity through Test Specimens

Test Specimen	Experimental Velocity (km/s)	Known Velocity (km/s)
Aluminum	3.1097	3.130
Pine	3.042	3.322
Cow bone	3.299	3.400
Cow soft tissue	1.472	1.540
Human bone	2.857	3.400
Human soft tissue	1.099	1.540



### 7.1 Results for Input Signal

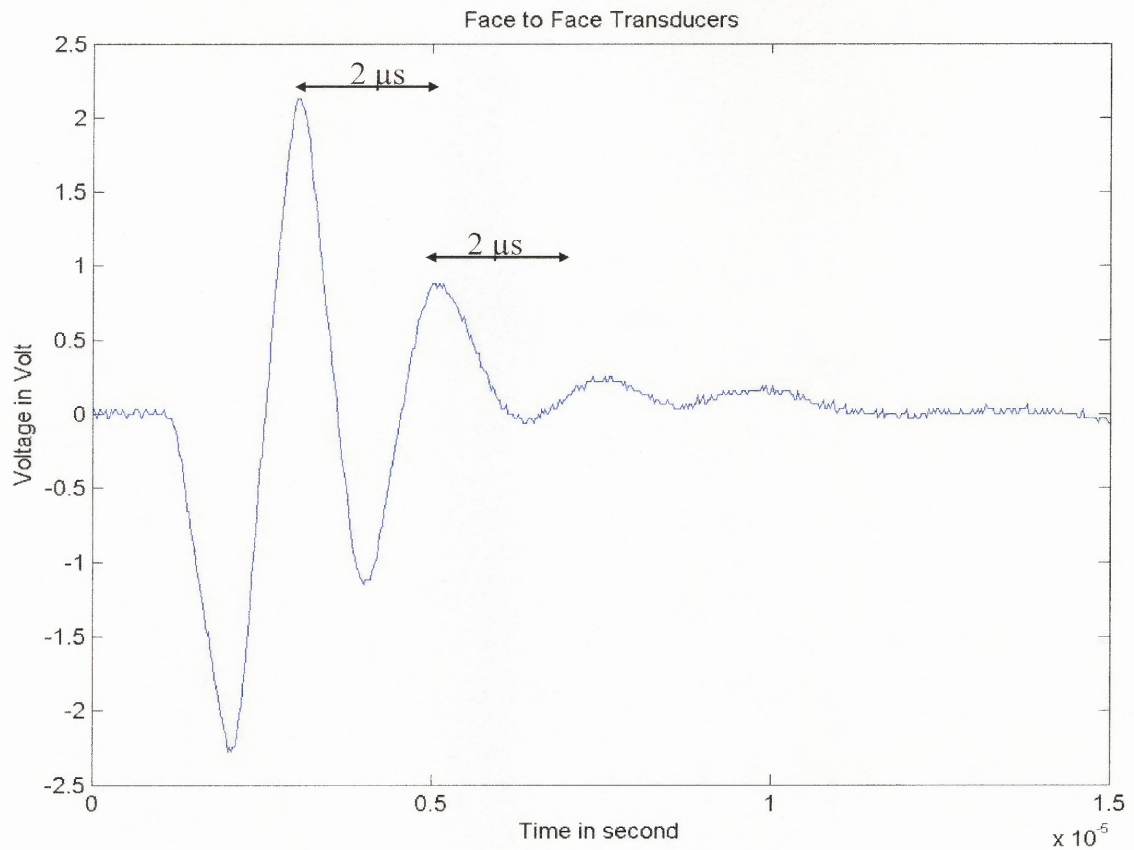


**Figure 7.1** Input signal waveform.

The input signal is generated by joining the transmitting transducer and a receiving transducer face to face. It has a consistent peak to peak amplitude of  $2 \mu\text{s}$ . This is the signal that goes into each of the waveforms obtained on the various test materials. This has helped in analyzing the received ultrasound signal.

## 7.2 Results for Wood

### 7.2.1 Wood without Cut versus Wood with Cut

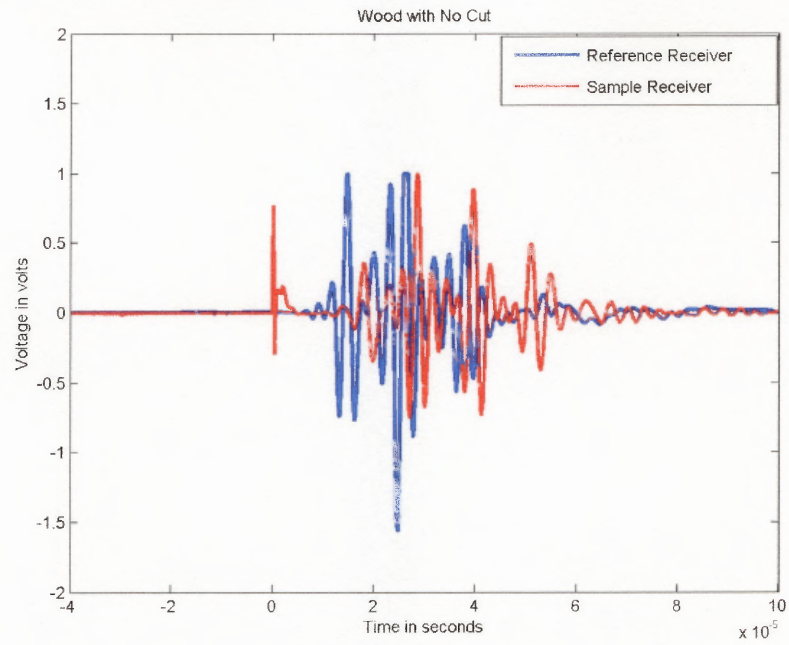


**Figure 7.2** Overlapping waveforms for test on wood with no cut.

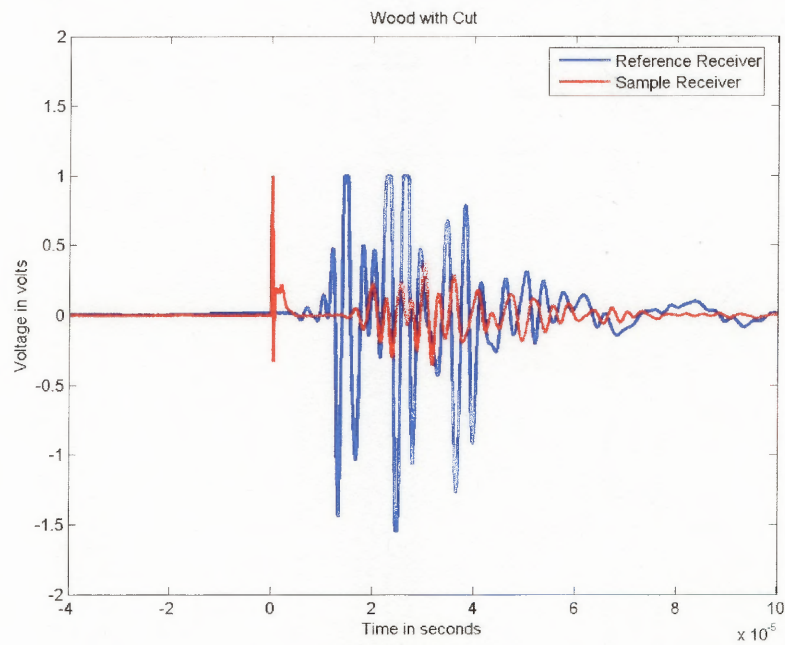


**Figure 7.3** Overlapping waveforms for test on wood with cut.

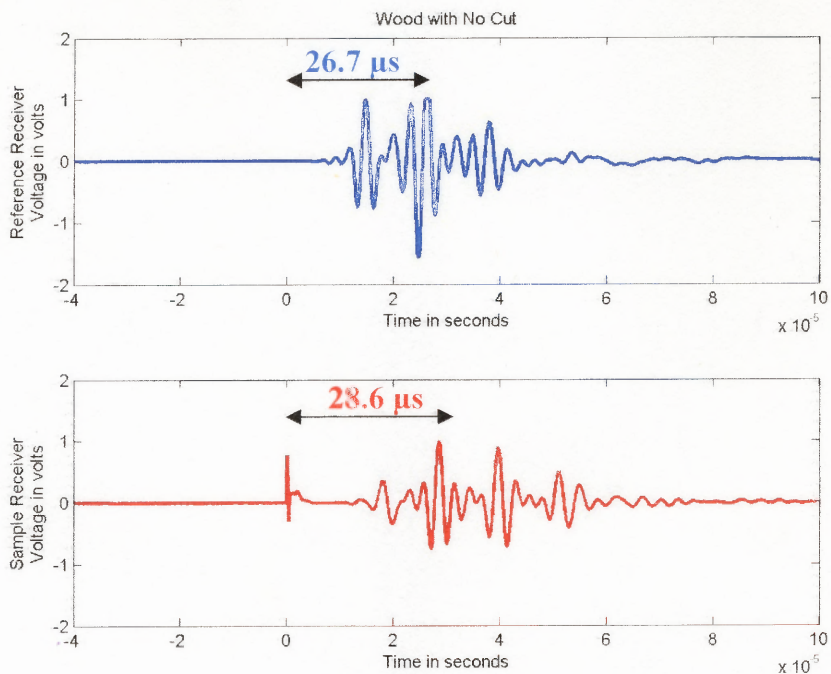


**Figure 7.4** Separated signals for test on wood with no cut.

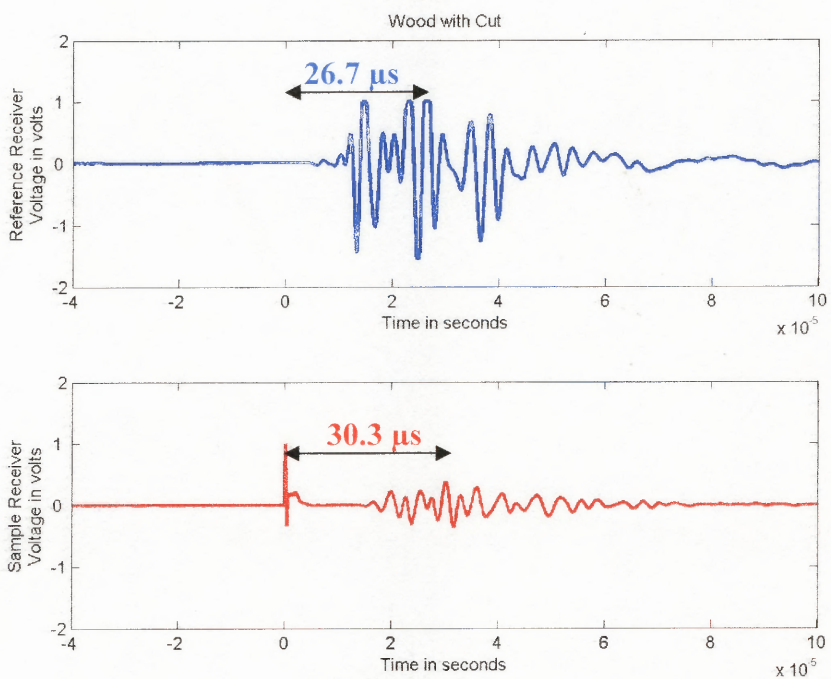


**Figure 7.5** Separated signals for test on wood with cut.



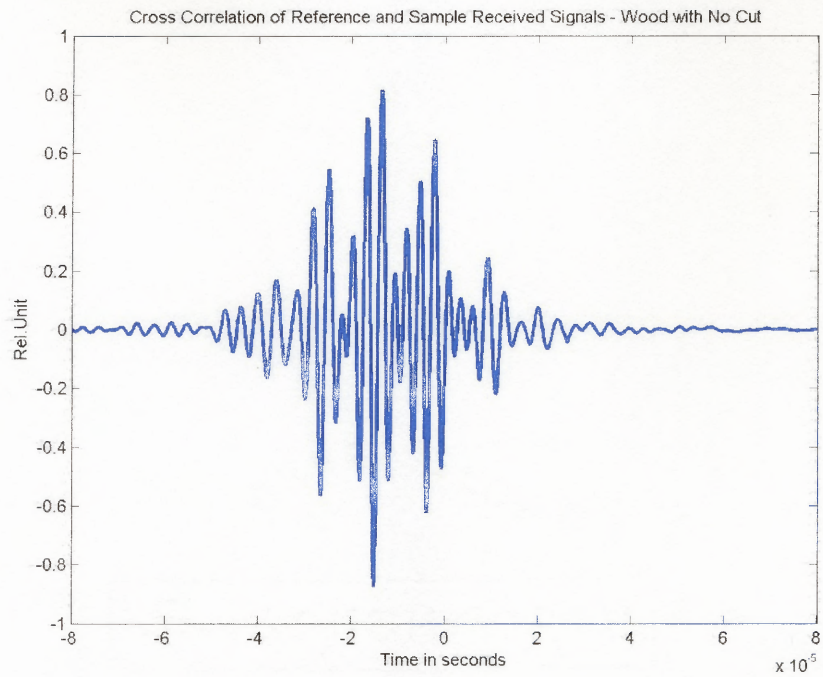


**Figure 7.6** Cross-correlation of received signals for wood with no cut.

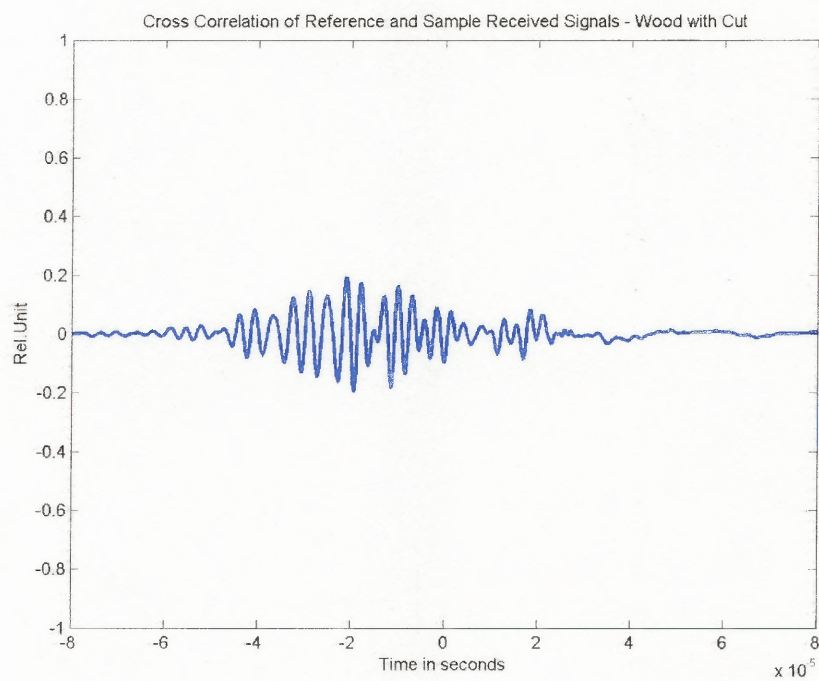


**Figure 7.7** Cross-correlation of received signals for wood with cut.

Figures 7.2 through 7.5 show the oscilloscope traces of the experiments conducted on the piece of wood. Flight time remains constant for the reference receiver at 26.7  $\mu\text{s}$ . As can be seen in Figure 7.4, when the transducers were placed over the section of wood with no cut, there is only a time delay in the received signal for the far (sample) receiver. The flight time increased from 26.7  $\mu\text{s}$  to 28.6  $\mu\text{s}$ . This occurs because the ultrasound has to travel a greater distance in order to reach the sample receiver as opposed to the reference receiver. The amplitude however, remains the same and so does the appearance of the shape of the signal.

When the two receivers are placed across a cut on the piece of wood, a greater difference in flight time and decrease in amplitude are observed. Flight time increases from the reference flight time of 26.7  $\mu\text{s}$  to 30.3  $\mu\text{s}$  and amplitude decreases from 1 V to 0.38 V. This is shown in Figure 7.5. This greater increase in flight time occurs because the ultrasound from the transmitting transducer has to travel around the cut in order to reach the sample receiver and get displayed on the oscilloscope.

Comparing the sample receiver signals of Figures 7.4 and 7.5, we can therefore see that flight time increases from 28.6  $\mu\text{s}$  to 30.3  $\mu\text{s}$ .

Finally, the cross-correlation Figures 7.6 and 7.7, clearly demonstrate that a large difference is seen between the received signals obtained from the experiment conducted over the piece of wood with no cut versus the piece of wood with a 2 mm deep cut across the two receivers.

Using the sample received signal in Figure 7.4, the velocity of ultrasound in wood is calculated as  $(0.087 \text{ m}) / (28.6 \mu\text{s}) = 3.042 \text{ km/s}$ .

## 7.2.2 Dowel of Wood and Wood with Knot

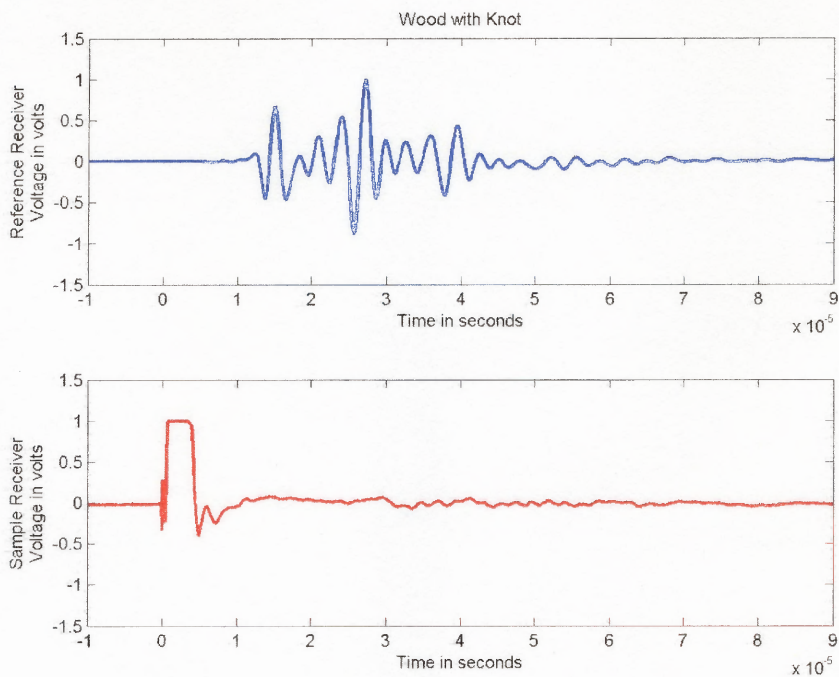


**Figure 7.8** Reference and received signals for wood with a knot on it.

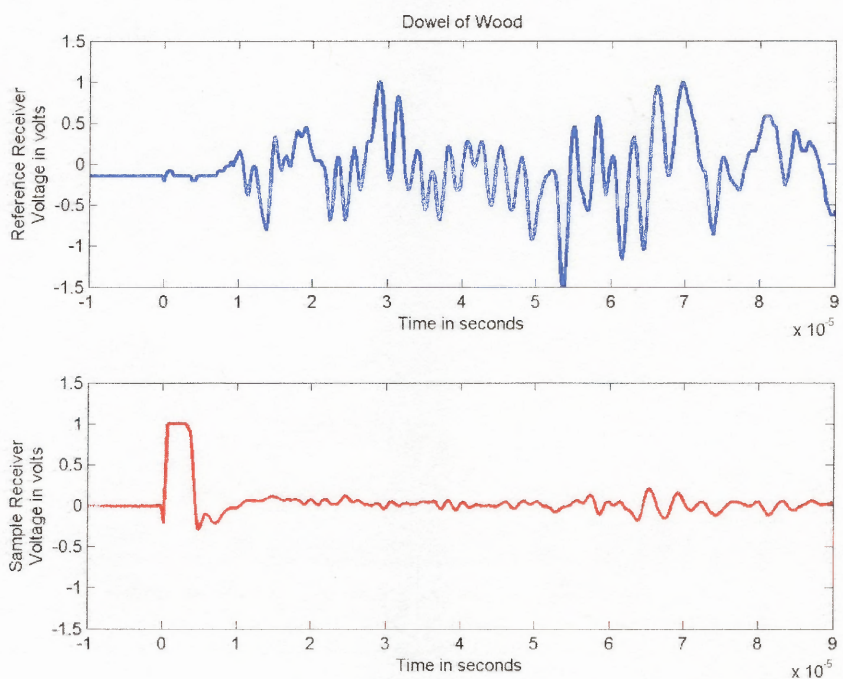


**Figure 7.9** Reference and received signals for a dowel of hardwood.

The results obtained from the piece of wood with a knot on it and from the dowel of wood show similar results. The response obtained from the sample receiver looks nothing like the reference signal in each case.

In the case of the wood with a knot, the knot can be treated as a defect in the piece of wood. There is a dramatic decrease in amplitude and flight time delay could not be measured.

In the case of the dowel, it shows that the transducers must be completely in contact with the test specimen. This calls for the need to use smaller transducers with the same specs to suit our needs.

Amplitudes are greatly reduced in both cases.

### 7.3 Results for Metal

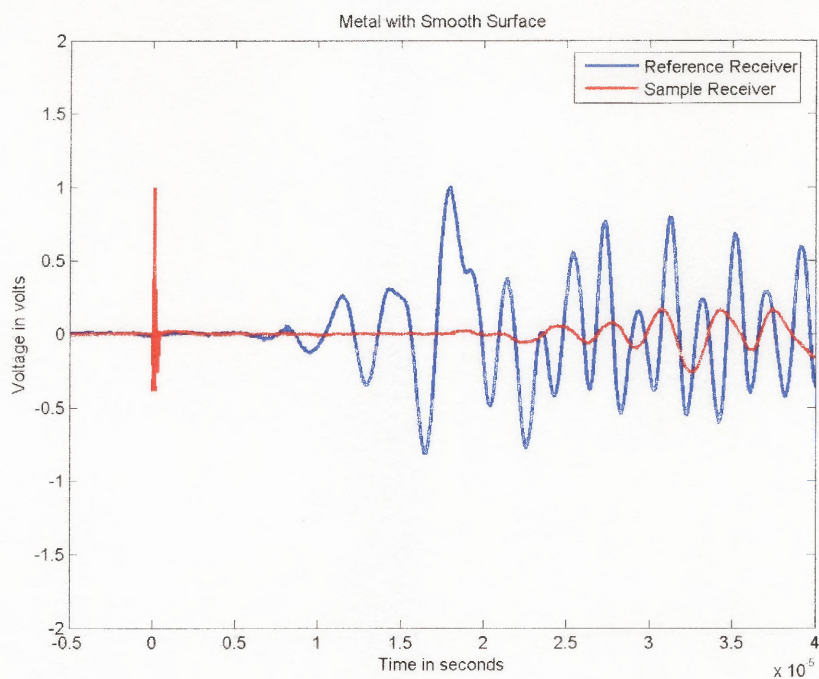


**Figure 7.10** Overlapping waveforms for test on metal without hole.

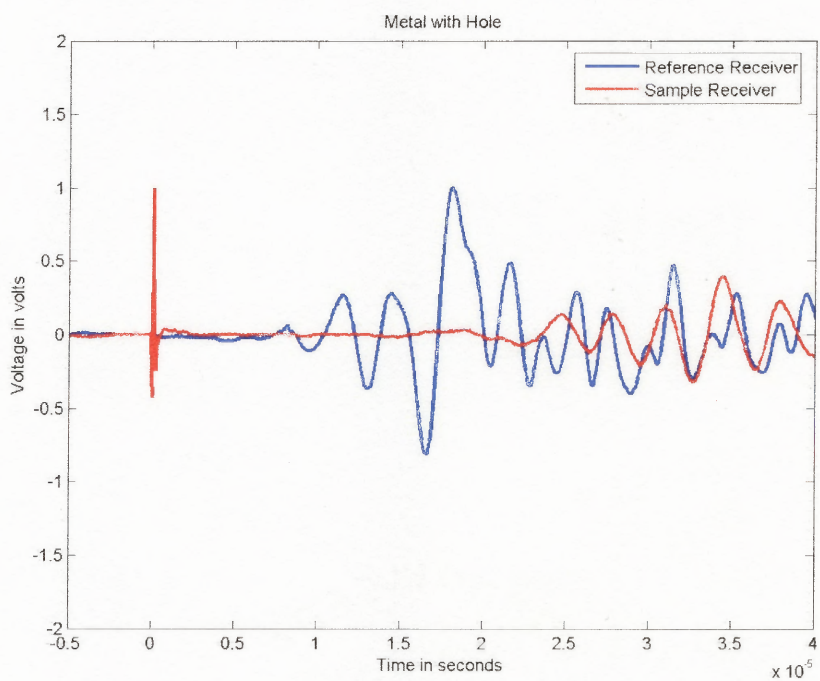


**Figure 7.11** Overlapping waveforms for test on metal with hole.



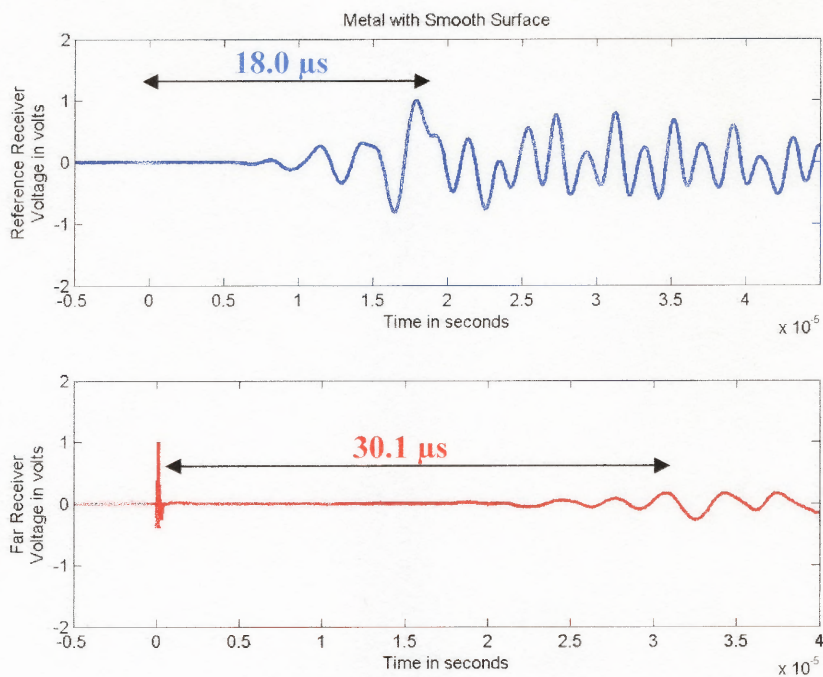


**Figure 7.12** Separated signals for test on metal without hole.

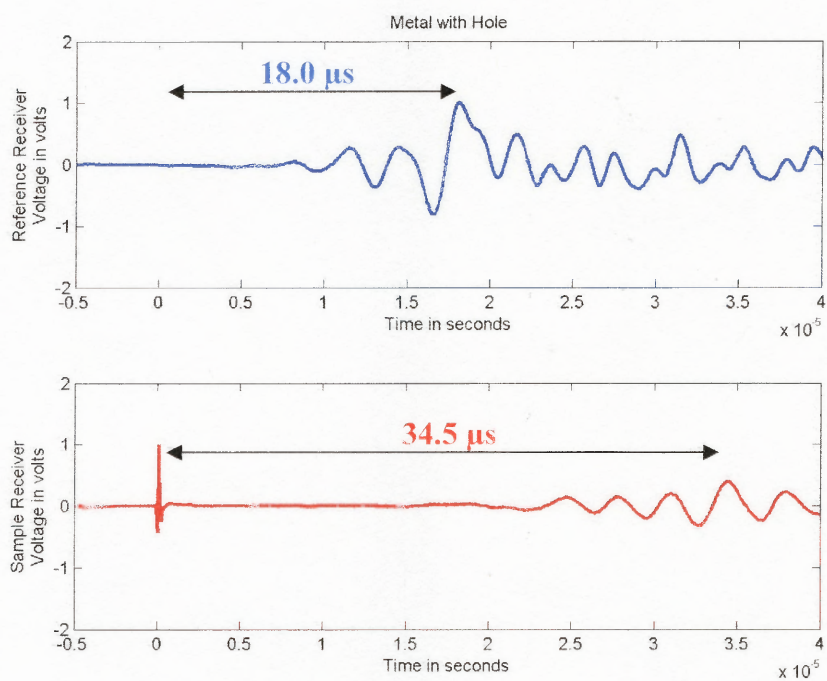


**Figure 7.13** Separated signals for test on metal with hole.

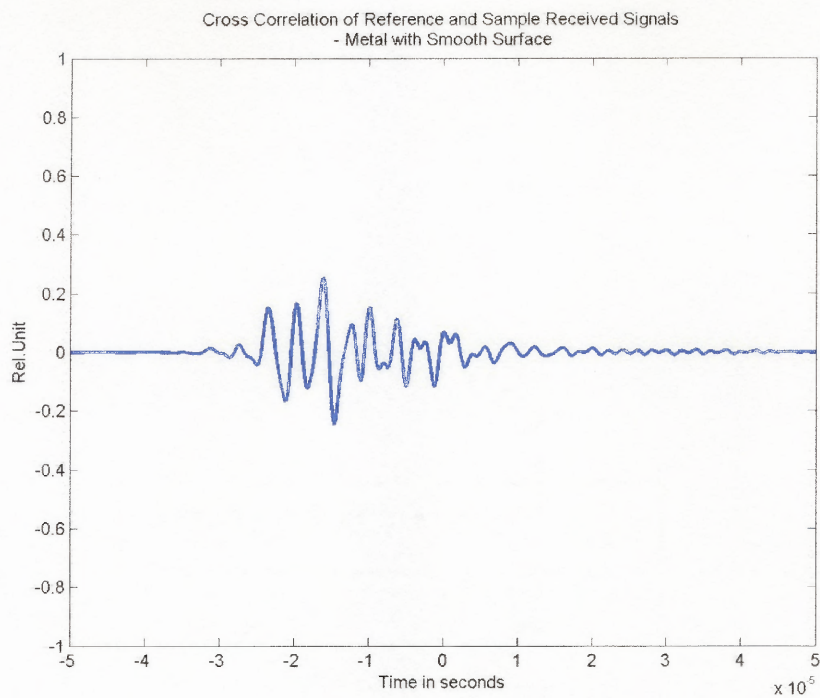


**Figure 7.14** Cross-correlation of received signals of metal without hole.

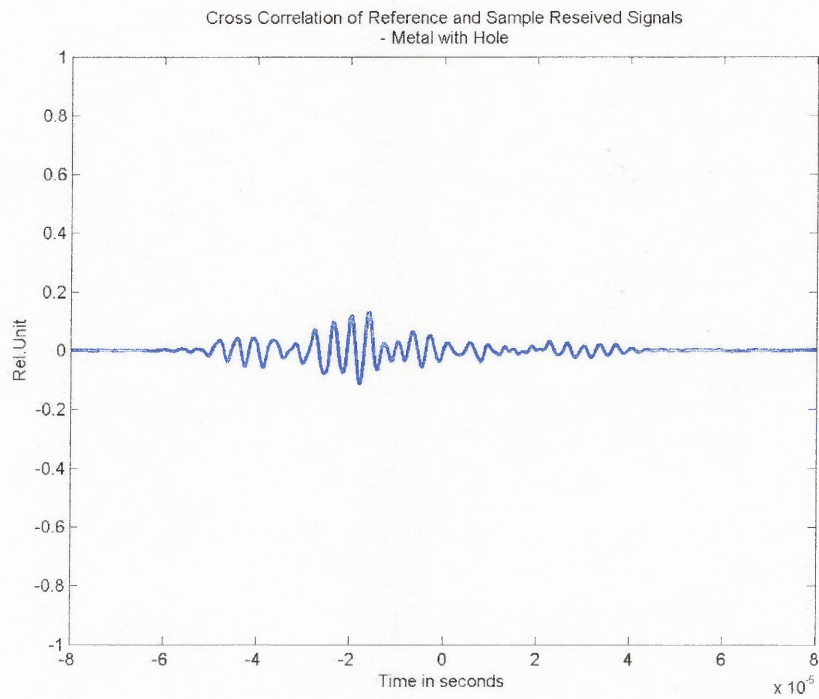


**Figure 7.15** Cross-correlation of received signals for metal with hole.

The results for the piece of metal (aluminum) are similar to those obtained from the wood experiments. The overlapping Figures 7.10 and 7.11 clearly show the increase in flight time of the sample receiver signal as opposed to the reference receiver signal. Figure 7.12 very evidently illustrates the flight time increase from 18.0  $\mu\text{s}$  in the reference receiver to 30.1  $\mu\text{s}$  in the sample receiver signal for the test across a smooth surface on the metal. Amplitude decreases from 1 V to 0.16 V.

Figure 7.13 shows flight time increase from 18.0  $\mu\text{s}$  in the reference receiver to 34.5  $\mu\text{s}$  in the sample receiver signal for the test across a hole. In this case, the amplitude decreases from 1 V to 0.13 V. Once again, the greater flight time occurs since the ultrasound has to travel around the hole in the aluminum and also because the sample receiver is farther away from the transmitting transducer than the reference receiver.

Just like the piece of wood, cross-correlating the two received signals in the case of the metal with hole versus no hole gives the same results of a drastic decrease in amplitude, as can be seen in figures 7.14 and 7.15.

Using the sample received signal in Figure 7.12, the velocity of ultrasound through aluminum is calculated to be  $(0.095 \text{ m}) / (30.1 \mu\text{s}) = 3.156 \text{ km/s}$ . This is extremely close to the actual velocity of ultrasound through aluminum, which is 3.130 km/s.

It is also noteworthy to observe that the signals in the case of the piece of metal have greater number of counts as opposed to those obtained from the piece of wood. This is attributed to the difference in modulus of each of these materials.

## 7.4 Results for Cow bone

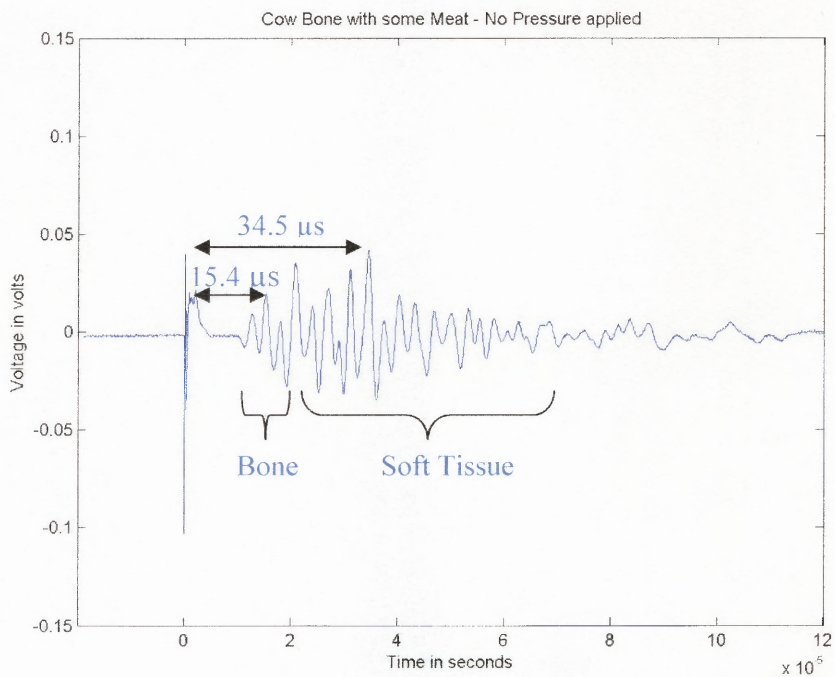


**Figure 7.16** Received signal for cow bone with no pressure.

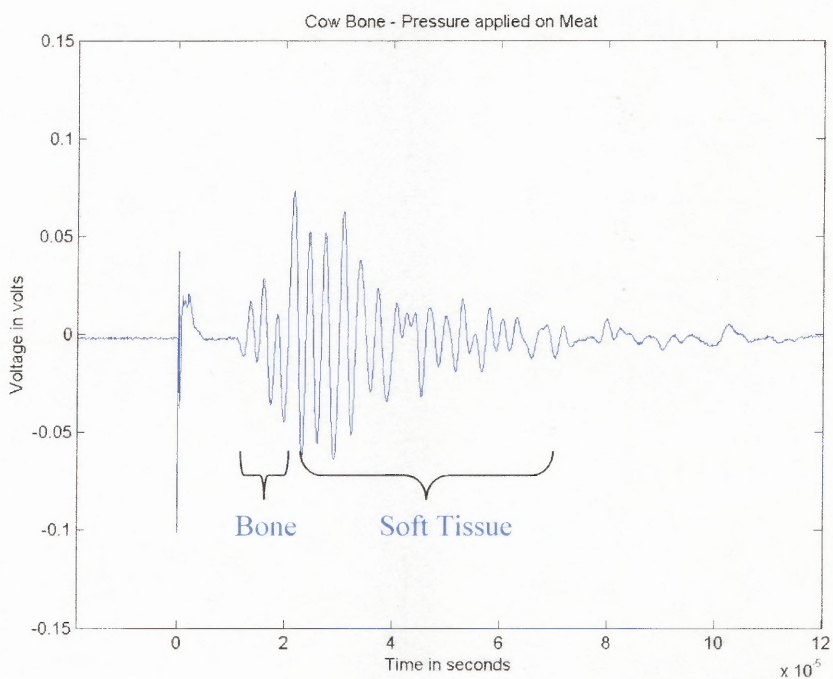


**Figure 7.17** Received signal for cow bone with pressure applied.

The experiments conducted on the cow bone have produced very interesting results. The received signal showed two almost distinct packets of signals. The first packet contained three spikes and the rest was assumed to be the second packet. Packet separation was confirmed due to the fact that when the meat on the cow bone was pressed, only the second packet showed disturbance and increased dramatically in amplitude (Figure 7.17) whereas the first packet remained stationary. This, in turn, implies that the first packet corresponds to the signals obtained when ultrasound traveled through the bone whereas the second packet corresponds to the soft tissue sticking on the piece of bone.

A theoretical fact for further confirmation of the fact that the first packet represents bone and the second represents soft tissue is that the speed of ultrasound through bone (3.400 km/s) is twice the speed of ultrasound through soft tissues (1.540 km/s). Therefore, it takes lesser time for ultrasound to travel through bone, which makes the bone response appear before the soft tissue response. This can be numerically shown by calculating the experimental value of ultrasound velocity through the two packets as follows.

Flight time of the first packet is 15.4  $\mu\text{s}$  whereas that of the second packet is 34.5  $\mu\text{s}$ . So the ultrasound velocity through the first packet is calculated as  $(0.051 \text{ m})/(15.4 \mu\text{s}) = 3.299 \text{ km/s}$  whereas ultrasound velocity through the second packet is calculated as  $(0.051 \text{ m})/(34.5 \mu\text{s}) = 1.472 \mu\text{s}$ . These values are therefore highly correlated.



## 7.5 Results for Human Arm

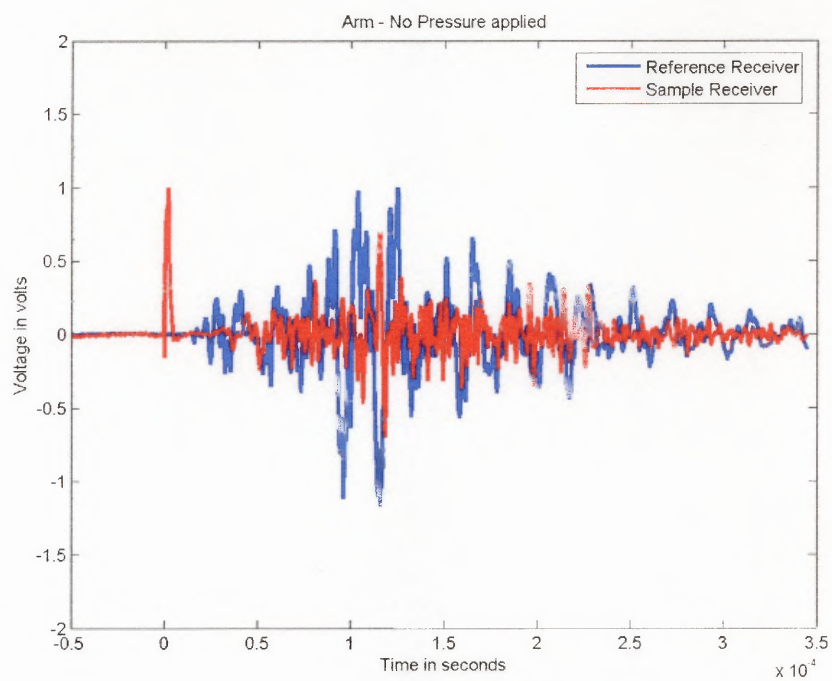


**Figure 7.18** Overlapping waveforms for arm with no pressure applied.

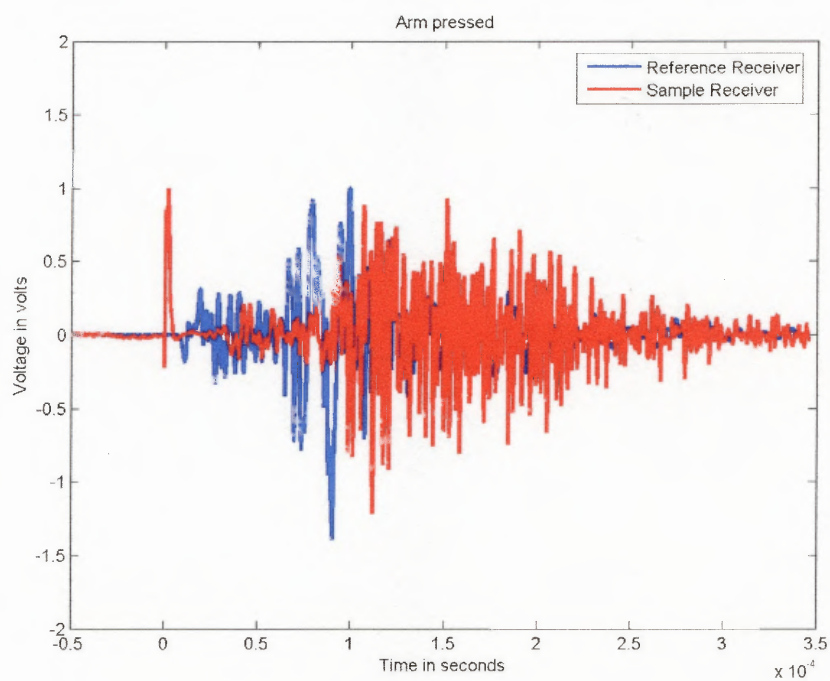


**Figure 7.19** Overlapping waveforms for arm with pressure applied.

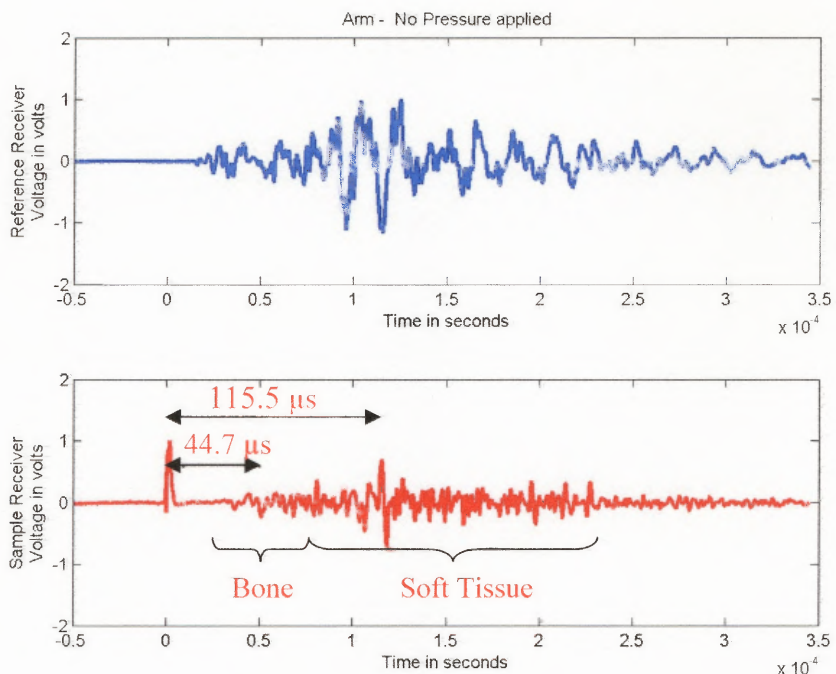


**Figure 7.20** Separated signals for test on human arm with no pressure applied.

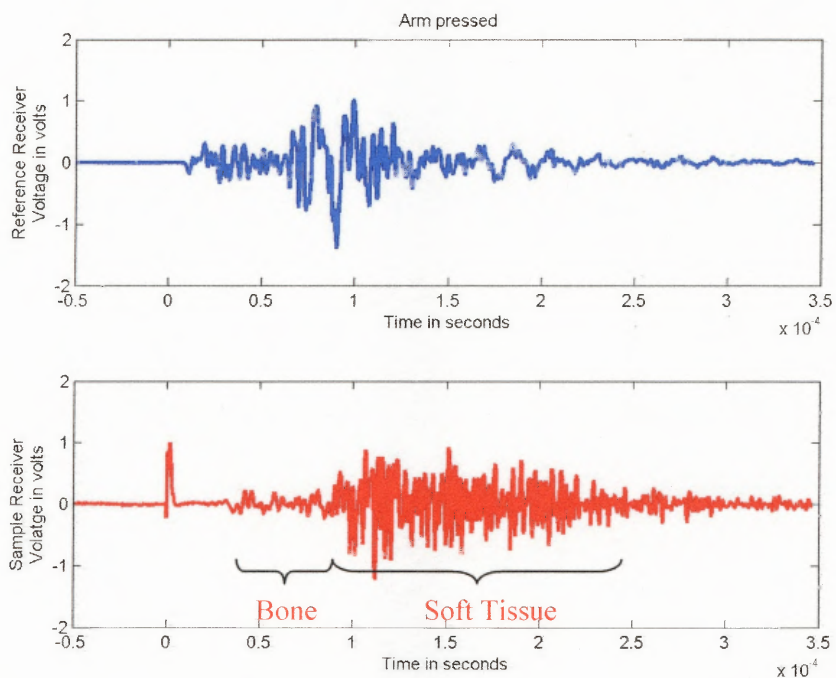


**Figure 7.21** Separated signals for test on human arm with pressure applied.

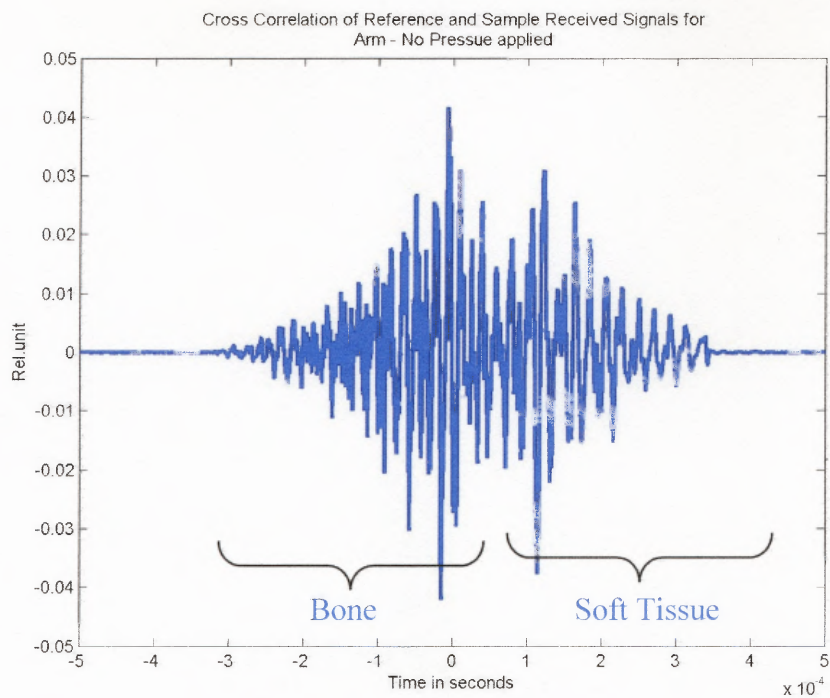


**Figure 7.22** Cross-correlation of received signals for arm with no pressure.

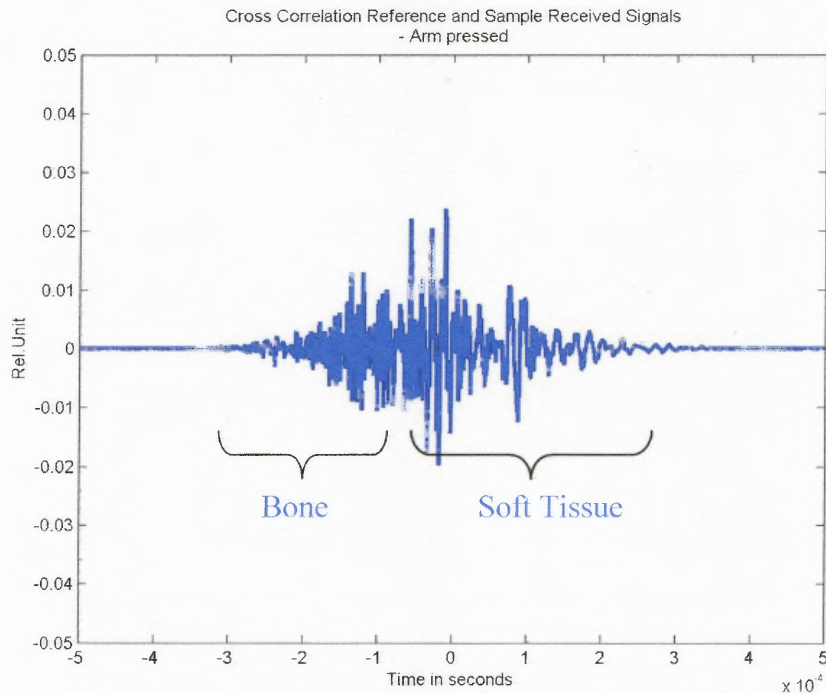


**Figure 7.23** Cross-correlation of received signals for arm with pressure applied.



Results for the human arm were similar to those obtained from the cow bone. Two packets of signals were obtained from each receiver, one representing bone and the other representing soft tissue around bone. The separation can be seen at around  $63 \mu\text{s}$  in the signal from the reference receiver in Figure 7.20 and  $90 \mu\text{s}$  in the sample receiver signal in Figure 7.21 when the arm is pressed around the transducers. This shift is expected due to greater distance traveled by the ultrasound.

The cross correlation waveform of the two received signals can be seen in Figures 7.22 and 7.23. The separation is not very evident when the arm is under normal conditions. This might be because these signals require some sort of filtering. However, when the arm is pressed, a slight separation is seen at about  $76.5 \mu\text{s}$ .

Once again, to further confirm the existence of two packets of signals, ultrasound velocities are calculated in each packet and are found to be very close to the actual velocity of ultrasound through bone and soft tissue. From Figure 7.20, flight time for the first packet is found to be  $44.7 \mu\text{s}$  whereas that of the second packet is  $115.5 \mu\text{s}$ . Therefore, the experimental ultrasound velocities are found to be  $2.857 \text{ km/s}$  and  $1.099 \text{ km/s}$  for the first and second packets respectively. They are close to the actual values and the difference can be attributed to varying moisture content in that particular bone.

## 7.6 Results for Human Tibia

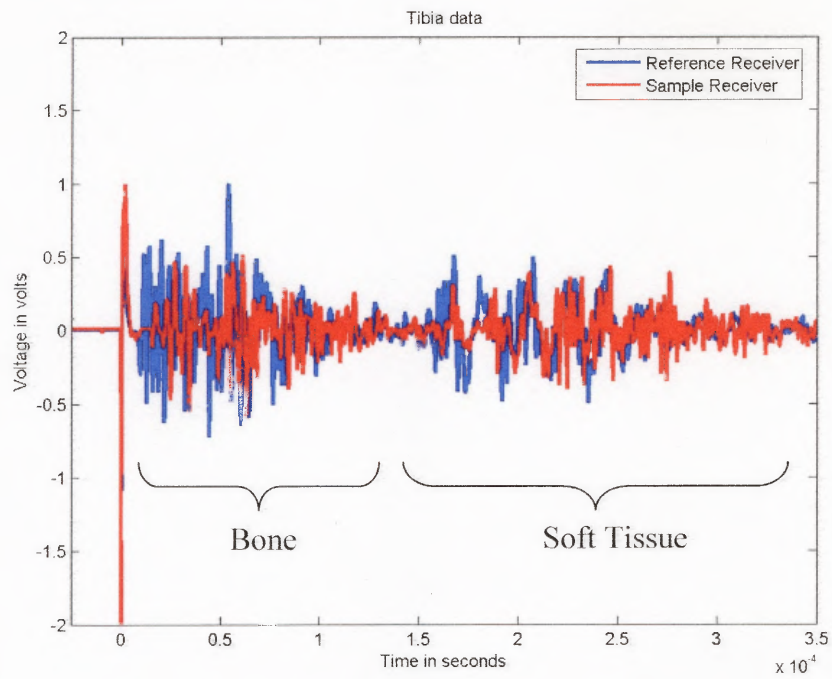


**Figure 7.24** Overlapping waveforms for test on the human tibia.

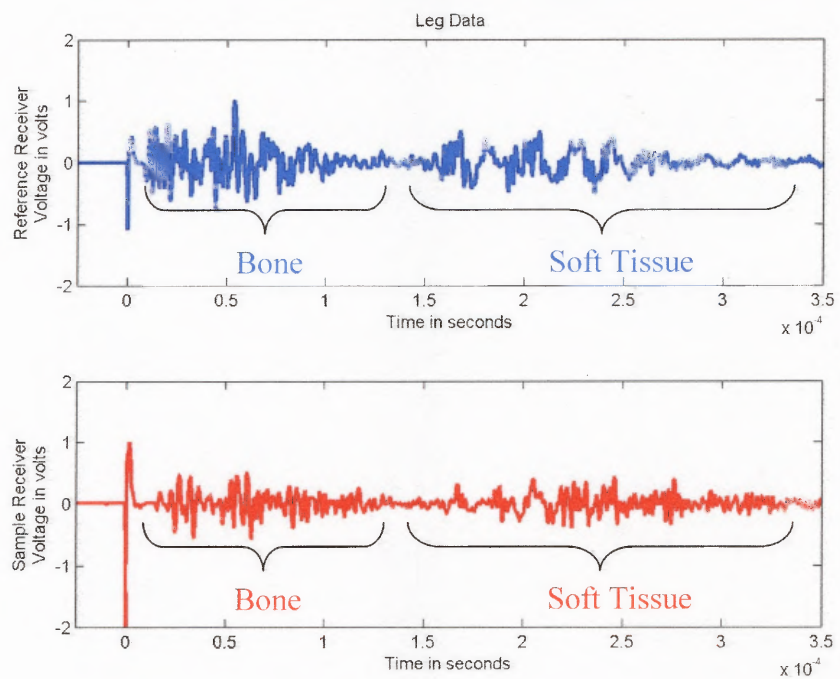


**Figure 7.25** Separated signals for test on the human tibia.

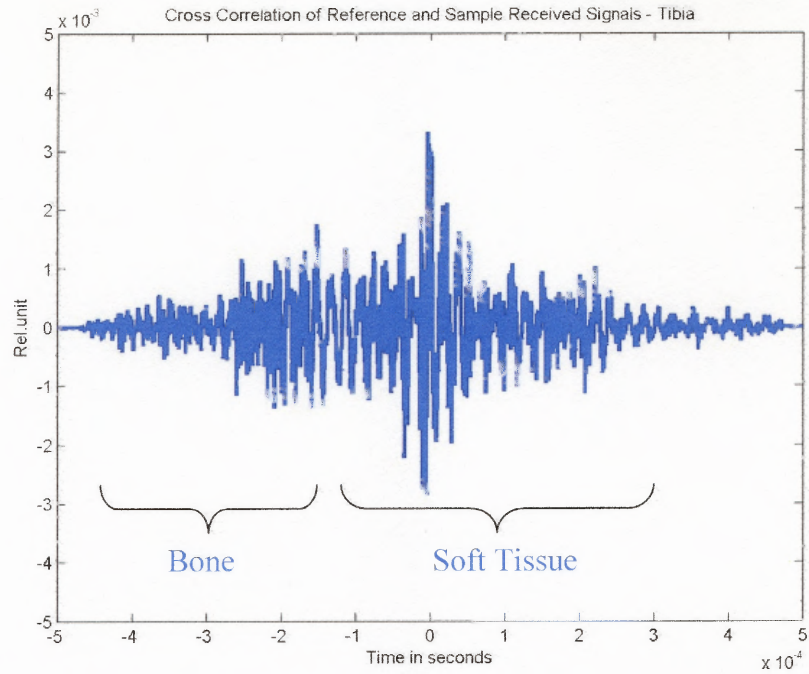


**Figure 7.26** Cross-correlation of received signals for tibia.

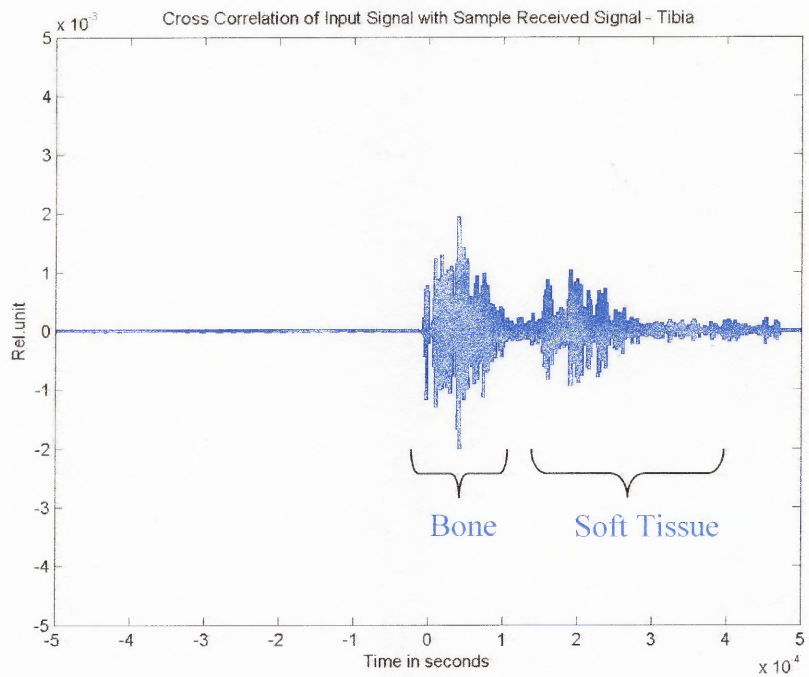


**Figure 7.27** Cross-correlation of input and far received signals for tibia.

The results obtained from the human tibia are perhaps the best ones obtained in this study. This is because, there is a very distinct separation between the two packets of signals. The slight delay of  $10\mu\text{s}$  in flight time from the reference receiver to the sample receiver is expected since the waves have to travel a greater distance. This is clearly seen in Figures 7.24 and 7.25.

The cross-correlation output (Figure 7.26) also shows some separation between the two packets. A better separation is seen by cross-correlating the input signal (Figure 7.1) with the reference received signal for the test on the tibia and this can be seen in Figure 7.27. This further confirms the fact that this technique can indeed be used for measuring mechanical integrity of long bones as well as soft tissue.

### 7.7 Result Summary

No change in the parameter being considered indicates healthy bone whereas with defect this value increases. As the bone starts healing, this value gradually comes back to zero. This is illustrated in Figure 7.28 below.

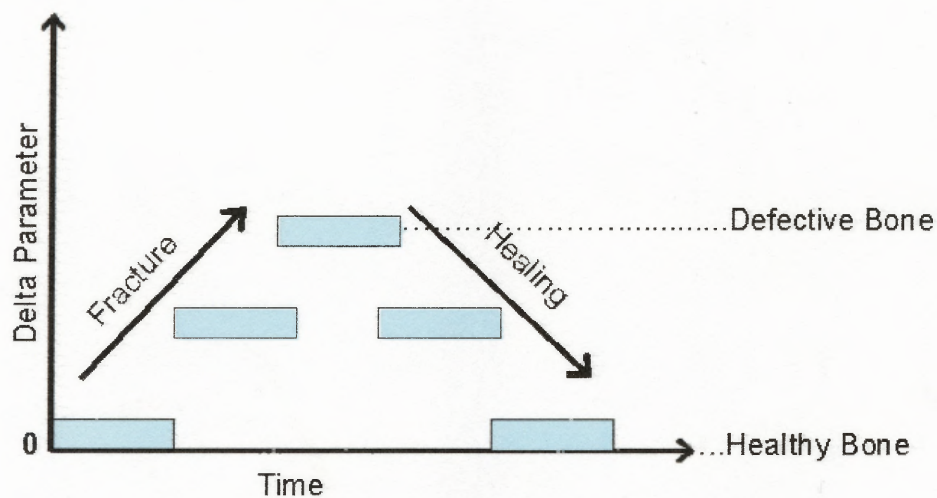


**Figure 7.28** Illustration of how delta parameter changes in the healing process.



## CHAPTER 8

### CONCLUSION

It has been shown that correlated ultrasound signals can be used to detect fracture and/or foreign inclusions in bones. This modern demonstration unit utilized serves as proof of principle for the device as originally defined in U.S. Patent # 5143069. The technique is non-invasive and sensitive to stress fractures or defects along materials like wood, aluminum, as well as bone and soft tissue. Sound waves transmitted through the suspected damage area translate into lines and peaks on a graph showing the location and the extent of an injury. The response is quantified in terms of flight time and amplitude. Defects make flight time go up and amplitude of the received signals to go down. Figure 8.1 depicts graphical representations of this outcome.

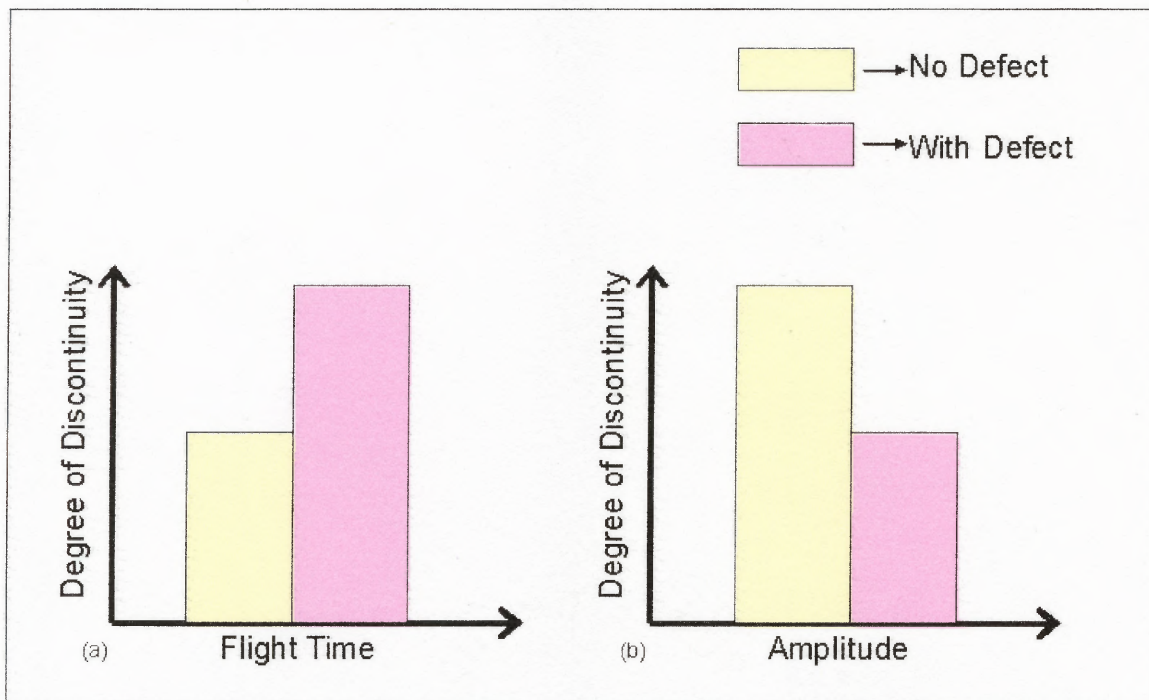


**Figure 8.1** Graphical representation of change in parameter with and without defect. (a) Flight time quantification. (b) Amplitude quantification.

Repeatability, sensitivity and spacing of the transducers are important factors that are taken into consideration. Repeatability is important because only if the obtained results are consistent can this be materialized into a commercial product. The sensitivity factor enhances the obtained responses. And the spacing between the transducers facilitates calculation of ultrasound velocity through the material being tested.

Besides detecting bone fractures, another application of this device would include monitoring the rate of bone healing over time. Since a defect increases flight time and decreases signal amplitude, a deeper cut would give a higher flight time value and a lower amplitude value than a less deep cut. Therefore, monitoring the bone healing process over a certain period would display how the flight time and amplitude of the received signals gradually come back to the value they deviated from when measured (Figure 7.28).

Yet another application can be monitoring soft tissues since two packets were observed in the case of cow bone and the human arm experiments. More complex bone abnormalities such as osteoporosis can also use application of this technique.

This device can therefore detect any type of defect such as a straight line cut, a hole-like defect, or even a knot-like defect. The first two resemble fractures whereas the latter can represent demineralization of bone due to osteoporosis or even bone tumor. On the whole, the device can tell the difference between a healthy bone and a damaged bone.

Sending high frequency sound waves through bone in this manner requires no radiation which poses no risk in checking repeatedly to plot the course of recovery. It is not only safe but saves time to a large extent as well.

It is a very promising technology and has great potential in developing into a portable device that can be taken “to” the patient as opposed to the other techniques used today that fall considerably short. It will be especially helpful to athletes, dancers, runners and other active people who want to know when they can safely resume strenuous exercise after encountering with a broken bone. The device would be relatively inexpensive and simple enough for doctors to use in their offices. These goals are anticipated keeping in mind the two main factors of reducing cost and improving healthcare by avoiding the harmful radiations that current fracture detecting technologies use.

## CHAPTER 9

### DRAWBACKS – NEEDS FOR THE NEXT GENERATION INSTRUMENT

The major drawbacks of this study were:

- There were distortions in the received responses of the tests on the arm and tibia. In order to eliminate that, a Fast Fourier Transform can be applied to the time domain waveforms for conversion into the frequency domain and back to the characteristic response with an Inverse Fast Fourier Transform, as indicated in the patent.
- The pulse generator used had only one built-in amplifier because of which only the far receiver signal was amplified. In order to compare the far receiver signals with the reference signals, the scales had to be adjusted in the scope each time an experiment was conducted. This can be overcome with the use of an extra external amplifier for the reference signal
- Since this device is designed to monitor long bone continuity, it would be very difficult to detect fractures on other bones such as the ribs. In that case, a linear array of miniature transducers fixed on a vest-like cuff would be an ideal solution.



## CHAPTER 10

### RECOMMENDATIONS AND FUTURE WORK

The following is a list of things that should be done to further develop the device:

- Energy should be the third parameter to measure the degree of discontinuity in the bone. Since  $\text{volt}^2\text{-sec}$  corresponds to units of energy, the y-axis of the cross-correlated waveforms obtained in this study can be normalized, squared and then the area under the curve can be taken to give the energy of that signal for a particular experiment. In this way, the change in energy can be measured over time and therefore serves as another important tool in this diagnostic process.
- In order to shrink the device to make it portable, much smaller transducers are necessary and the other devices (pulse generator, digital oscilloscope) need to be configured into a single unit and displayed on a PDA (Personal Digital Assistant). This would be an important step in taking the device to the patient instead of the other way around.

## REFERENCES

1. Contact Ultrasonic Transducers Technical Notes (2005). [Document posted on the Website of Panametrics-NDT]. Retrieved April 15, 2005 from the World Wide Web: [http://www.panametrics-ndt.com/ndt/ndt\\_transducers/downloads/transducer\\_technotes.pdf](http://www.panametrics-ndt.com/ndt/ndt_transducers/downloads/transducer_technotes.pdf)
2. Bone Fracture. [Document posted on the Website of Mama's Health, Lakewood, California]. Retrieved on November 10, 2005 from the World Wide Web: <http://www.mamashealth.com/bodyparts/fracture.asp>.
3. Bone Fracture. [Document posted on the Website of Wikipedia, The Free Encyclopedia]. Retrieved on November 13, 2005 from the World Wide Web: [http://en.wikipedia.org/wiki/Fracture\\_%28bone%29](http://en.wikipedia.org/wiki/Fracture_%28bone%29).
4. Merriam Webster Online. [Document posted on the Website of Merriam Webster]. Retrieved on November 15, 2005 from the World Wide Web: <http://www.m-w.com/>.
5. The Big Story on Bones. [Document posted on the Website of Kids Health]. Retrieved on December 1, 2005 from the World Wide Web: [http://kidshealth.org/kid/body/bones\\_noSW.html](http://kidshealth.org/kid/body/bones_noSW.html).
6. The Skeletal System. [Document posted on the Website of The Human Body]. Retrieved on December 2, 2005 from the World Wide Web: <http://users.tpg.com.au/users/amcgann/body/skeletal.html>.
7. Gustafsson, L., Jacobson, B., & Kusoffsky, L. (1974). X-ray spectrophotometry for bone-mineral determinations. Medical and Biological Engineering, 12, 113-119.
8. Well, P.N.T. (1977). Biomedical Ultrasonics. Medical Physics Series, 124-130.
9. Yoon, H.S., Caraco, B., Kaur, H., & Katz, J.L. (1980). Clinical Application of Acoustic Emission Techniques to Bone Abnormalities. 1980 Ultrasonics Symposium Proceedings (IEEE), 1067-1072.
10. Yoon, H.S., Caraco, B., Kaur, H., Katz, J.L., & Michelli, L.J., (1981). Non-Invasive and Non-Traumatic Diagnosis of Bone Abnormalities by AE techniques, Proceedings of the Institute of Acoustics.
11. Rondinone, P. (1982). Listening to Bones. Continuum, 42.
12. Meunier, A., Yoon, H.S., & Katz, J.L. (1982). Ultrasonic Characterization of some Pathological Human Femora. 1982 Ultrasonics Symposium Proceedings (IEEE), 713-715.

13. Stephen Kiesling. (1982). Bone Listening to Stop Injury. American Health Vol.1, No.2, May/June, 54
14. Yoon, H.S. (1983). Applications of a New Acoustic Emission Technique to Head Injuries. Department of Biomedical Engineering, Rensselaer Polytechnic Institute, Troy, New York.
15. Yoon, H.S., & Katz, J.L. (1983). Is Bone a Cosserat Solid? Journal of Material Science, 18, 1297-1305.
16. Yoon, H.S. (1985). Bone Strength Measuring System based on Acoustic Emission. Department of Biomedical Engineering, Rensselaer Polytechnic Institute, Troy, New York.
17. Kwon, S.J., Yoon, H.S., & Katz, J.L. (1985). Increased Sensitivity in the Non-Invasive Acoustic Emission Technique for Bone Fracture Diagnosis. 1985 Ultrasonics Symposium Proceedings (IEEE), New York, 864-867.
18. Kwon, S.J., & Katz, J.L. (1986). Sonic Diagnosis of Bone Fracture and Diseases: Time Series and Frequency Analysis. Ultrasonics Symposium Proceedings (IEEE), New York, 949-952.
19. Kwon, S.J., & Katz, J.L. (1987). Sonic Diagnosis of Skeletal Defects: A Preliminary Study. Advances in Dental Research. Orthosonics Inc, New York and Department of Biomedical Engineering, Rensselaer Polytechnic Institute, Troy New York, 39-44.
20. Perre, G.V.D, & Lowet, G. (1996). In Vivo Assessment of Bone Mechanical Properties by Vibration and Ultrasonic Wave Propagation Analysis. Bone Vol. 18, No. 1, Supplement, 29S-35S.
21. Chen, T., Chen, P.J., Fung, C.S., Lin, C.J., & Yao, W.J. (2004). Quantitative Assessment of Osteoporosis from the Tibia shaft by Ultrasound Techniques. Medical Engineering & Physics, 26, 141-145.
22. Kwon, S.J., & Katz, J.L. (1982). Diagnostic Method of Monitoring Skeletal Defect by In-Vivo Acoustic Measurement of Mechanical Strength using Correlation and Spectral Analysis. United States Patent # 5143069.
23. Speed of Sound Through Materials. (2002) [Document posted on the Website of U.K Piano Pages; Association of Blind Piano Tuners]. Retrieved December 10, 2005 from the World Wide Web: <http://www.uk-piano.org/sound.html>.